WSRC-TR-2004-00418

TANK 5 MODEL FOR SLUDGE REMOVAL ANALYSIS

Si Young Lee

Westinghouse Savannah River Company
Savannah River Site
Aiken, SC 29808

Prepared for the U.S. Department of Energy under Contract No. DE-AC09-96SR18500

WSRC-TR-2004-00418

KEYWORDS:
Sludge Suspension
Computational Approach
Slurry Jet Model
Maximum Clearing Distance

TANK 5 MODEL FOR SLUDGE REMOVAL ANALYSIS

Si Young Lee

September 2004

Westinghouse Savannah River Company
Savannah River Site
Aiken, SC 29808

Prepared for the U.S. Department of Energy under Contract No. DE-AC09-96SR18500

(This Page Intentionally Left Blank)

This page was intentionally left blank

(This Page Intentionally Left Blank)

Table of Contents

(This Page Intentionally Left Blank)

List of Figures

(This Page Intentionally Left Blank)

List of Tables

(This Page Intentionally Left Blank)

Abstract

Computational fluid dynamics methods have been used to develop and provide slurry pump operational guidance for sludge heel removal in Tank 5. Flow patterns calculated by the model were used to evaluate the performance of various combinations of operating pumps and their orientation under steady-state indexed and transient oscillation modes. A model used for previous analyses has been updated to add the valve housing distribution piping and pipe clusters of the cooling coil supply system near pump no. 8 to the previous tank Type-I model. In addition, the updated model included twelve concrete support columns. This model would provide a more accurate assessment of sludge removal capabilities. The model focused on removal of the sludge heel located near the wall of Tank 5 using the two new slurry pumps. The models and calculations were based on prototypic tank geometry and expected normal operating conditions as defined by Tank Closure Project (TCP) Engineering.

Computational fluid dynamics models of Tank 5 with different operating conditions were developed using the FLUENT™ code. The modeling results were used to assess the efficiency of sludge suspension and removal operations in the 75-ft tank. The models employed a three-dimensional approach, a two-equation turbulence model, and an approximate representation of flow obstructions. The calculated local velocity was used as a measure of sludge removal and mixing capability.

For the simulations, modeling calculations were performed with indexed pump orientations until an optimum flow pattern near the potential location of the sludge heel was established for sludge removal. The calculated results demonstrated that the existing slurry pumps running at 3801 gpm flowrate per nozzle could remove the sludge from the tank with a 101 in liquid level, based on a historical minimum sludge suspension velocity of 2.27 ft/sec. The only exception is the region within maximum 4.5 ft distance from the tank wall boundary at the west corner of the tank.

Further results showed that the capabilities of sludge removal were affected by the presence of twelve concrete support columns, the indexed pump orientation, the number of operating pumps, and the pump flowrate. The major impact of the results for the presence of the 2-ft support columns is that the sludge cleaning distance is reduced by about 1.5 ft, compared to the model with no support columns. However, the impact of the cleaning distance for the presence of 2-in cooling coil pipe clusters near the pump nozzle is found to be negligible. Sensitivity results showed that for a given tank level and pump location, a higher pump flowrate would result in better performance in suspending and removing the sludge. The results also showed that the presence of flow obstructions such as concrete support columns were advantageous for certain pump orientations in terms of guidance of the flow direction.

1 Introduction

Tank 5 is a 0.75 million-gallon, single-wall, Type I waste tank located in the F-Tank Farm area. The tank was placed into service as a receiver of high heat wastes. The tank is a 75 ft diameter, flat-bottomed, cylindrical carbon steel tank with a height of about 24.5 ft. There are cooling coils, a valve housing to control coolant flow in the cooling coils, and 12 structural support columns internal to the tank. The waste in the tank consists of salt and sludge. The salt was removed by dissolution in water and transferred to other tanks for storage. The remaining sludge layer settled near the bottom will then be hydraulically mobilized and transferred to other tanks.

To mobilize the sludge layer and to suspend the settled sludge, water is added to Tank 5 as a slurry medium, and the Slurry Mixer Pump (SMP) is used to suspend the sludge [1]. Tank 5 with 75 ft diameter has two new slurry pumps manufactured by Curtiss Wright Electro-Mechanical Corp. available for sludge removal operations. The new pump is unique since the pump motor has been designed to be submerged inside the tank instead of being mounted on the tank top. The two pumps are located in the 75-ft tank as illustrated in Fig. 1. Each pump has a screened suction inlet at the bottom and two opposing discharge nozzles, 4.4 in. in diameter as shown in Fig. 2. The pump is normally submerged to approximately the level of the sludge, allowing a recirculating mixture of sludge and water to serve as the feed flow. The pump nozzle can not be placed lower than about 24 inches above the tank bottom [1]. The minimum nozzle elevation corresponds to about 16 inches from the tank floor to the bottom of the pump suction inlet as shown in Fig. 1.

Recent video inspections of Type-I tanks showed that some Type-I tanks such as Tank 3, 7, 8, 11, have valve house distribution piping above the free surface of waste in the tank, but the others including Tank 5 have it inside the waste liquid region [5]. All Type-I tanks have twelve 2-ft concrete support columns inside the tank. Schematic of the Tank 5 system as modeled for the present analysis is shown in Fig. 1. Each pump can rotate between 0.2 and 0.5 rpm (0.3 rpm used for the nominal Tank 5 analysis) using a variable frequency drive. The cleaning pattern generated on the tank bottom defines the effective cleaning radius (ECR) when the pump rotates. The ECR has been one of the measures or indicators of the cleaning ability of a mixing pump. After the mixer suspends the sludge, waste transfers from Tank 5 to another tank will be performed. Detailed design and operating conditions for the Tank 5 slurry pump are shown in Table 1.

In previous work for the Tank 18 mixing analysis [5], a three-dimensional computational fluid dynamics (CFD) model for a prototypic tank was developed and benchmarked against TNX test data. The test data were obtained from a mixing experiment conducted in a full tank mockup in the TNX area. The test tank was 85 ft in diameter and 8 ft high. The advanced design mixing pump of Tank 18 was used to suspend a kaolin clay slurry in the tank. Recently, the first-of-a-kind pump for the Tank 5 mixing operation has been tested in the full tank mockup in the TNX area using the slurry simulant of kaolin clay to ensure it performs to the work scope's specifications. This pump motor has been designed to be submerged inside the tank instead of the existing pump motor being mounted on the tank top. Its long shaft was enclosed in a 18 in nominal pipe diameter casing. The new submersible mixer pump to be used for the Tank 5 sludge removal is shown in Fig. 2. It was located 16 ft from the tank wall with a discharge elevation 24 in above the tank bottom. Kaolin clay slurries were used to simulate the actual sludge in the waste tanks [5]. The slurry contains about 25 wt% kaolin B-100 powders in water.

The primary objective of the present work is to provide an operational guideline for sludge removal in Tank 5. The flow patterns calculated by the model will be used to evaluate the capabilities of the slurry mixers under various combinations of two operating pumps and their nozzle discharge orientation. Schematic layout and dimensions of the Tank 5 sludge removal system to be modeled for the present work are shown in Fig. 1. Figure 3 shows the typical flow development and evolution of a jet flow discharged by a slurry mixer obtained from previous modeling results [4, 5] and literature information [11].

The analysis results will be used to evaluate hydraulic cleaning capabilities for waste removal. This information will also assist in the operating plan for the Tank 5 waste removal and in identifying special operation requirements for the suspension and removal of the tank sludge.

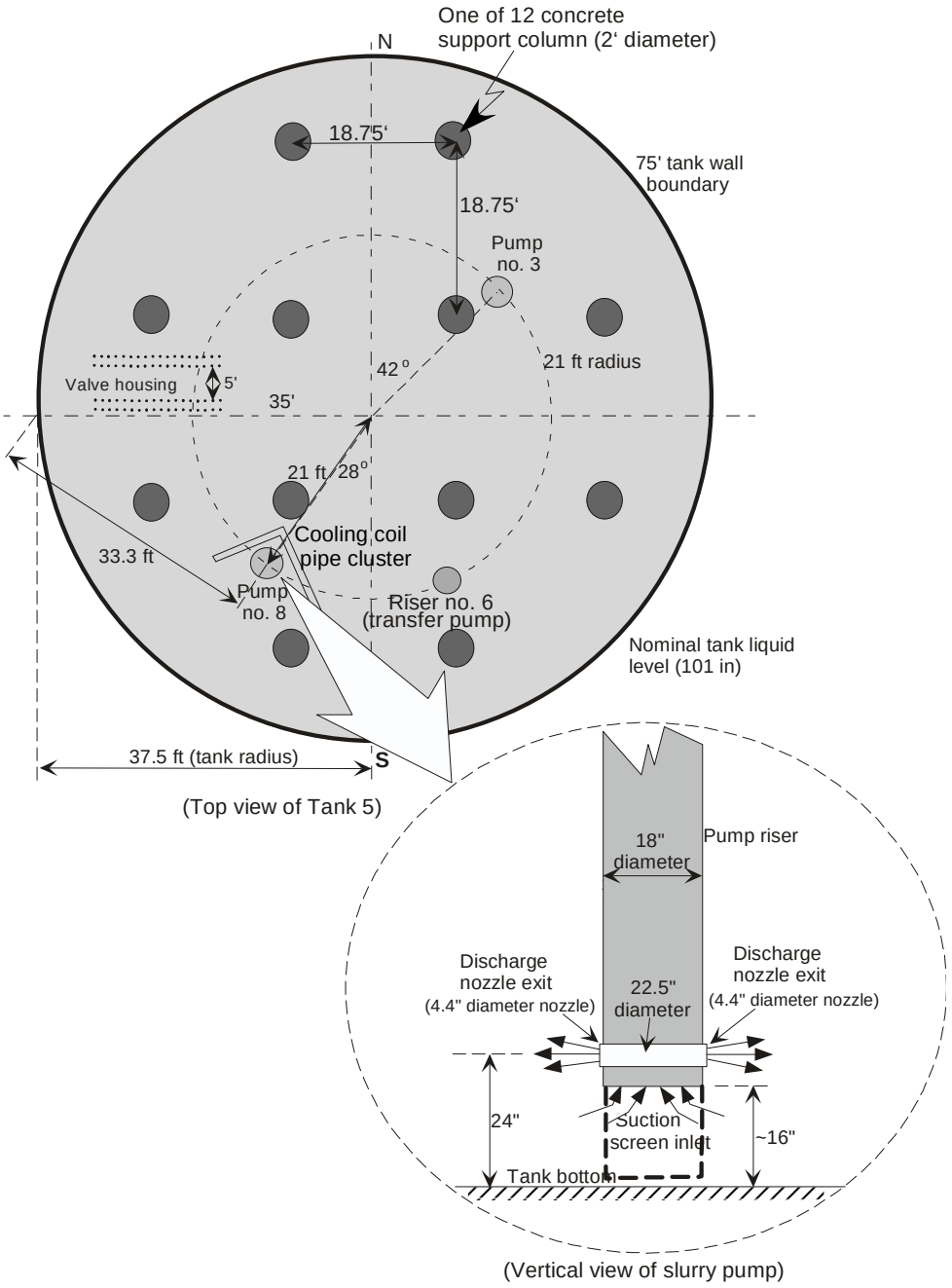

Figure 1. Schematic of Tank 5 layout with major flow obstructions of twelve concrete support columns, valve housing distribution pipe, cooling coil pipe cluster, and two slurry mixing pumps.

Figure 2. New submersible mixer pump to be used for the sludge removal operations in Tank 5 (Photo taken at TNX during kaolin testing)

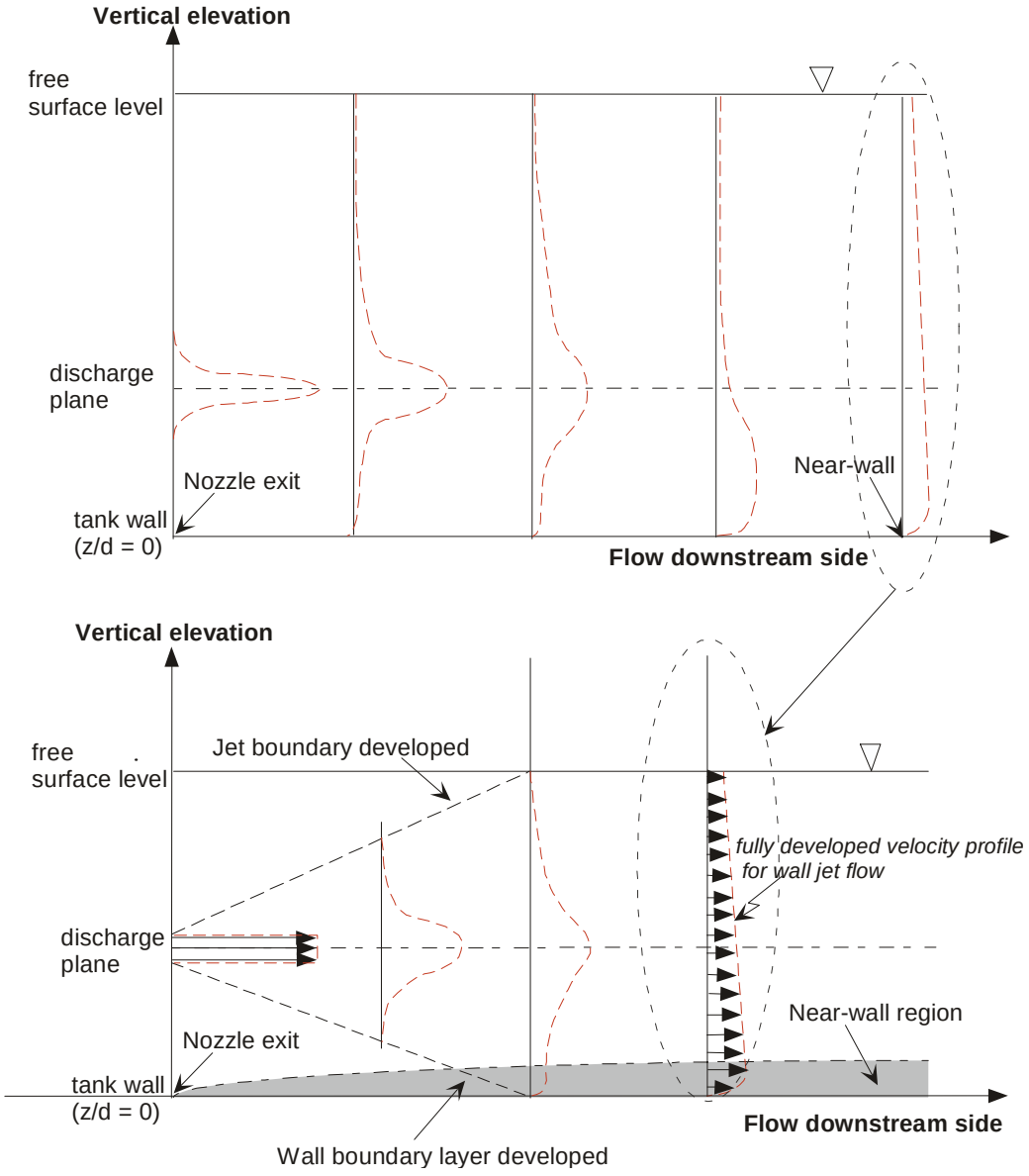

Figure 3. Typical velocity profiles in the direction perpendicular to the free surface from the modeling results of large-scale tank mixing simulations.

Table 1. Specifications of Tank 5 slurry pump used for the present analysis.

Design Parameters	Slurry Pump
Horsepower, hp	305
Pump casing diameter, inches	22.5
Pump column diameter, inches	18
Number of discharge nozzles (flow directions)	2 (180^o apart and opposite flow direction)
Nozzle diameter, inches	4.4
Pump suction location	Bottom of pump
Suction diameter, inches	14
Flowrate per nozzle, gpm	3801*
Flow velocity at pump discharge nozzle, ft/sec	About 64 (3040 gpm)
	About 80 (3801 gpm)*
	About 88 (4156 gpm)

Note: *Reference operating conditions (Pump speed for 3801 gpm flowrate is not determined yet.)

2. Modeling Approach and Analysis Method

A three-dimensional CFD approach is used to calculate flow patterns for the sludge removal operations of Tank 5 and to evaluate sludge removal capabilities for the tank. The calculation results were benchmarked against both TNX and literature data in the previous work [5]. The model predictions were in good agreement with test data and operational observations. The same finite volume CFD code, FLUENT [7], was used here to perform the Tank 5 modeling and analysis. A prototypic geometry is modeled by a non-orthogonal and hexahedral mesh combined with hybrid grid. The modeling domain to be used for the present analysis is presented in Fig. 4. Nominal design and operating conditions of the Tank 5 model are presented in Table 2.

The present models consider flow obstructions such as key pump support structures, 12 concrete support columns, 1 submersible transfer pump, second SMP, and pipe clusters associated with the cooling coil return and supply system inside the tank, but they do not model the presence of the sludge layer. Following the previous methodology [6], the flow velocity in the vicinity of the sludge heel is used as an indicator of the ability of the flow to suspend sludge and remove the heel.

Table 2. Reference design and operating conditions of Tank 5 used for the present analysis.

Parameters		**Conditions**
Tank dimensions	Diameter	75 ft
	Tank liquid level	101 in*, 70 in, and 45 in
Concrete support column diameter		2 ft
Mixing pump		A new slurry pump with pump motor submerged as shown in Fig. 2
Number of pumps		1 or 2*
Pump nozzle diameter		4.4 in
Pump operating mode		Indexed* or oscillating ($\pm 200^{o}$ with 1/3 rpm rotating speed)
Pump positions inside the tank	Vertical elevations	24 in (from the center of pump discharge nozzle to tank bottom)
	Horizontal locations	See Fig. 1
Tank fluid temperature		50^{o}C
Tank fluid		Water*, slurry+ (density: 1.2 SG, viscosity: 2 cp)
Nozzle flowrate for each nozzle [fluid speed]	3040 gpm	[64.2 ft/sec]
	3801* gpm	[80.2 ft/sec]
	4156 gpm	[87.7 ft/sec]

Note:* Reference operating conditions as provided by the customer [1, 2]
+ Water (50^{o}C) was used as a simulant for the present analysis, but slurry was used in the sensitivity analysis.

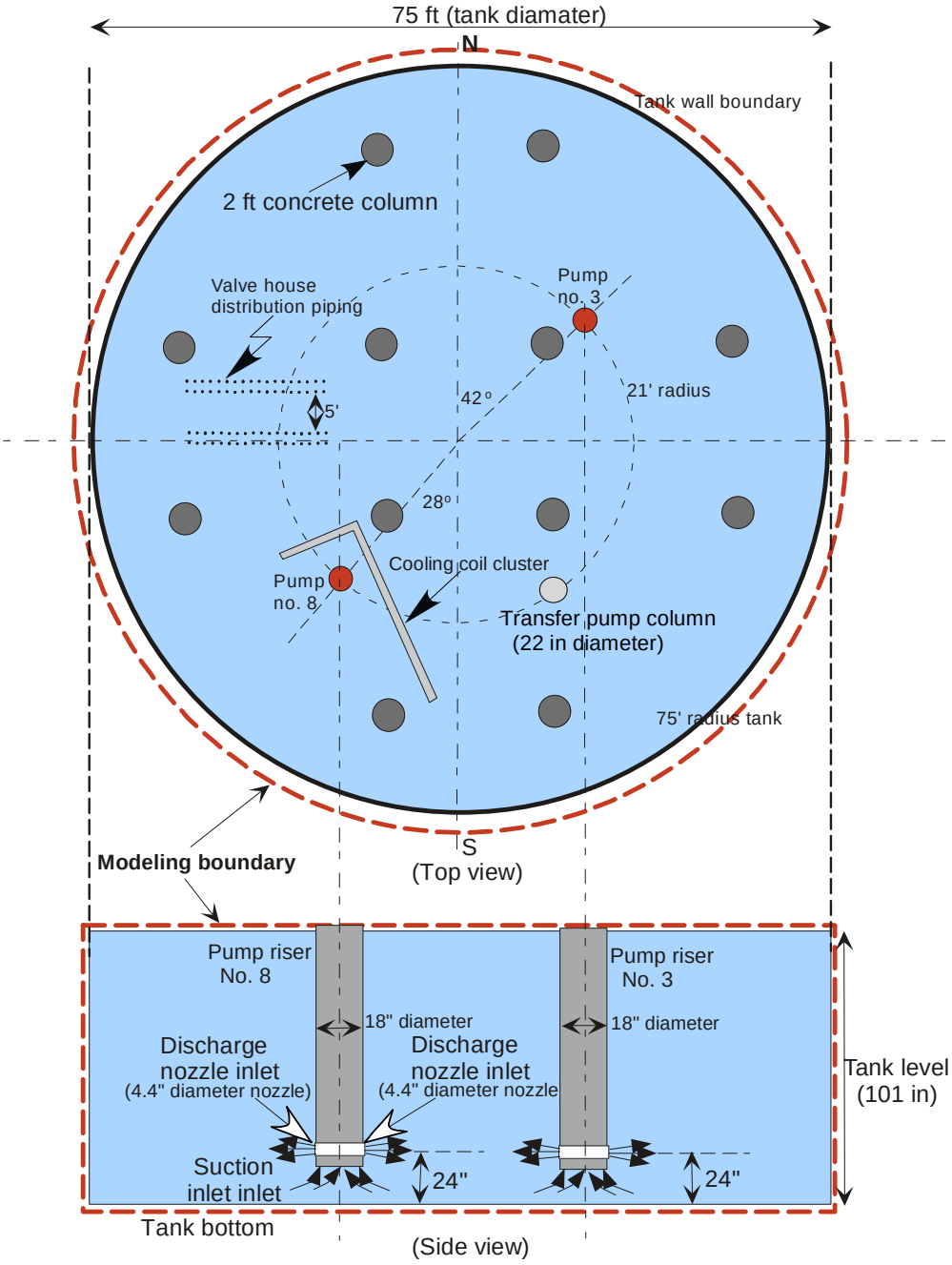

Figure 4. Three-dimensional modeling boundary for the present analysis of the Tank 5 facility with two slurry pumps

The focus of the present work is suspending sludge particles with the turbulent jet generated by a new submersible pump. Prior to discussing the CFD modeling approach, the literature results for a free turbulent jet flow are reviewed briefly, since the free jet flow is similar in many respects to the bounded wall jet. The previous work [2] and the literature data [3] show that when a turbulent jet of fluid is discharged from a nozzle with a diameter d_o, it both entrains fluids and expands. Most mixing action and entrainment takes place in the region of fully-developed flow which begins at a distance of approximately eight nozzle diameters from the exit plane. The non-dimensional velocity distribution φ_v along the jet axis of this region for a homogeneous fluid jet is given by [3]

$$\varphi_v = \left(\frac{v(x)}{U_o}\right) = C_o\left[\frac{x}{d_o}\right]^{-1} = C_o\,\eta^{-1} = K\eta^{-1} \qquad (1)$$

In Eq. (1), C_o is a constant determined by the turbulence characteristics of the jet, U_o the nozzle exit velocity, $v(x)$ the local velocity at a point *x*, and *x* the distance from nozzle. Abramovich (1963) correlated experimental data for a free turbulent jet submerged in fluid using the non-dimensional form provided by Eq. (1). From his work for free jet without any flow obstructions, the proportionality constant C_o in Eq. (1) was determined to be 6.32. Since the pump discharge flow inside large-scale tanks at SRS is affected by the bottom of the tank and internal flow recirculation, the constant *K* is evaluated from the previous Tank 18 calculations rather than classical free jet theory. It was found to be 4.874 [5]. The maximum axial velocity at any axial position *x* can be estimated using Eq. (1). The equation shows that the velocity at any point in the region of established flow is directly proportional to the product, d_oU_o. Thus, the axial entraining distance corresponding to minimum entrainment velocity can be estimated with nozzle diameter and flow rate.

The fluid domain for Tank 5 has both a solid wall boundary and a free surface boundary as the jet expands into the downstream region and ultimately recirculates via the suction on the bottom of the pump as shown in Fig. 1. The spreading fluid is retarded by the interaction with the wall as shown in Fig. 3, and the inner part of the flow may be expected to show a certain structural similarity to a boundary layer. Entrainment of quiescent fluid occurs near the outer edges of the flow, and accordingly resembles a free jet [14]. In this case sludge particles settled near the edge of the boundary region are entrained into a turbulent zone, and they are suspended. Estimations of minimum suspension velocity, particle settling rate, and incipient erosion velocity will be discussed for establishment of a flow velocity criterion in the subsequent sections.

2.1 Estimation of Suspension Velocity During Mixing Operation

The decay of the axial jet velocity and the evolution of flow patterns are important phenomena affecting sludge suspension and mixing operations. A measure of the ability to shear the sludge layer, the scouring wall shear, is directly related to the local fluid velocity. The initial movement of solids deposited on the bottom of the tank identifies the critical condition or initial scour. It is usually described by two criteria, the minimum flow velocity and the frictional shear to scour and initiate movement of deposited solids particles. From these two criteria, a local fluid velocity can be determined as a performance indicator for adequate suspension.

When liquid flow passes over a settled sludge layer containing small solid particles, the flow results in hydrodynamic forces being exerted on individual particles in the layer. The initial movement of the top of the sludge layer is called the critical condition of suspension. The degree of suspension resistance for a given particle to the hydrodynamic forces of the flowing fluid depends on the cohesion and adhesion forces. An increase in the fluid momentum causes an increase in the magnitude of the hydrodynamic forces. Hence, for a particular stationary sludge layer, a condition is eventually reached at which particles in the movable bed are not able to resist the hydrodynamic forces and solids in the top layer start to lift.

Average flow velocity, particle size and density, and slurry flow regime are key important parameters in determining the transport patterns of particles in a slurry [16], which are closely related to the solid resuspension. In this case, the critical velocity is defined as the minimum velocity that can initiate the movement of the solids deposited near the bottom of the tank. Graf [16] correlated the critical velocity V_c empirically in terms of geometrical dimensions and the ratio of particle to fluid densities using data available in the literature.

$$V_c = \left(\frac{d}{H}\right)^{-0.1} \sqrt{2.5gd\left(\frac{\rho_s}{\rho_f} - 1\right)} \qquad (2)$$

In Eq. (2) d and H are the particle diameter and tank liquid level, respectively. As seen in Fig. 5, when the average flow velocity is much larger than the critical velocity, V_c, the literature results show that solid particles in a continuous flow field are homogeneously distributed [16]. When the flow velocity required for sludge transport and suspension is exceeded, the solid-laden flow can be treated as a homogeneous fluid. Thus, once solid particles are suspended by the continuous-phase flow, the conditions of the first of the three typical slurry flow fields shown in Table 3 are satisfied. The present flow calculations are based on a homogeneous single-phase fluid flow. Table 3 shows minimum suspension velocities of particles for three different mono-sized particle systems with 2.5 specific gravity (spg) particle and 1.2 spg fluid under different tank levels. The flow criterion required for sludge suspension will be used in the analysis as shown in Table 3.

Table 3. Minimum velocities of particle suspension and transport/removal for the various particle sizes in fluid density 1.2 spg (particle density=2.5 spg)

Tank level (inches)	Sludge particle size (microns)	Min. velocity (V_c) required to suspend particle deposited on horizontal wall surface computed by Eq. (2) [cm/sec] (ft/sec)
101*	1	[2.26] (0.074)
	10	[5.67] (0.186)
	60*	[11.58] (0.380)*
70	1	[2.16] (0.071)
	10	[5.46] (0.179)
	60*	[11.19] (0.367)
40	1	[2.04] (0.067)
	10	[5.15] (0.169)
	60*	[10.58] (0.347)

Note:* The present modeling calculations will use these values as the nominal reference conditions.

* Size of very fine sand = 60 microns

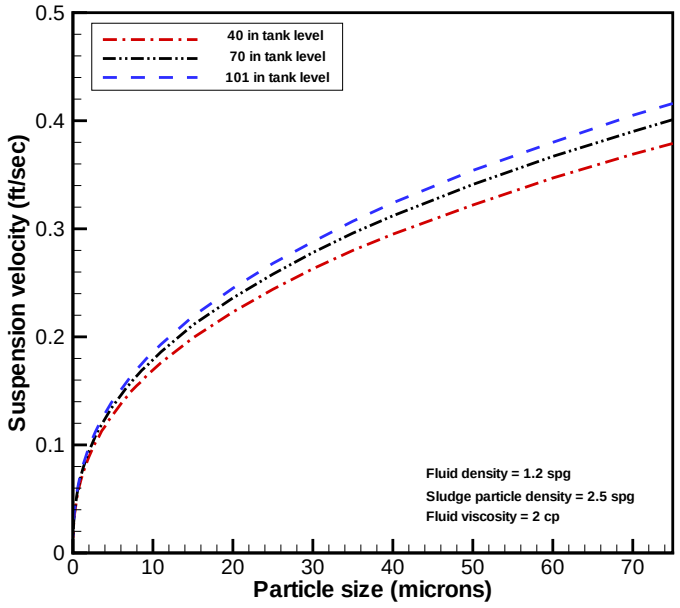

Figure 5. Sludge suspension velocity as function of particle sizes for different tank levels

2.2 Settling Velocity for Mono-sized Particles in Stagnant Fluid

The drag force on an isolated solid particle moving in an infinite expanse stagnant fluid is represented by the equation,

$$F_D = \frac{1}{2} C_D \rho_f v_f{}^2 A_p \tag{3}$$

In Eq. (3) ρ_f is density of fluid. A_p represents the projected cross-sectional area of the particle perpendicular to the direction of motion. C_D is the drag coefficient at the surface of particle when a solid particle is falling downward with velocity v_f. The drag coefficient C_D is dependent on particle shape and flow regime in terms of Reynolds number (*Re*).

For the case of settling of free particles of spheres at a constant velocity with a density of ρ_p and without interaction or hindering effects due to the presence of other particles, the drag force F_D equals the force of gravity F_G, including the buoyancy force of the particle with solid volume V_p submerged in a quiescent fluid.

$$\begin{aligned} F_G &= V_p (\rho_p - \rho_f) g \\ &= F_D \end{aligned} \tag{4}$$

After some algebraic manipulations, eqs. (3) and (4) become

$$v_f = \left[\left(\frac{2}{C_D} \right) \left(\frac{V_p}{A_p} \right) g \frac{(\rho_p - \rho_f)}{\rho_f} \right]^{0.5} = \left[\left(\frac{2}{C_D} \right) \varphi g \frac{(\rho_p - \rho_f)}{\rho_f} \right]^{0.5} \tag{5}$$

When the particle has a spherical shape with diameter d_p, the ratio (φ) of the particle volume to its projected area in Eq. (5) is (2/3)d_p. That is,

$$v_f = \left[\left(\frac{4}{3 C_D} \right) d_p g \frac{(\rho_p - \rho_f)}{\rho_f} \right]^{0.5} \tag{6}$$

In this situation, the flow is assumed to be slow viscous or Stokes's flow. In 1850, Stokes derived the solution for viscous flow past a sphere at small values of the Reynolds number by using the momentum equation without inertia terms in a spherical polar coordinate system and by fitting no-slip boundary conditions at the spherical surface. His result for drag force acting on the sphere was:

$$F_D = 3 \pi \mu_f d_p U_o \tag{7}$$

where U_o is the undisturbed free stream velocity.

When the particle velocity relative to the bulk fluid is equal to the undisturbed free stream velocity in Eq. (7) and Re < 0.6, the drag coefficient C_D in Eq. (5) corresponding to the Stokes formula, Eq. (7), can be expressed as

$$C_D = \frac{F_D}{\frac{1}{8} \rho_f v_f{}^2 \left(\pi d_p{}^2 \right)} = \frac{24}{Re} \tag{8}$$

The Reynolds number, *Re,* the dimensionless parameter used in Eq. (8), is defined in terms of particle size d_p and velocity v_f relative to the fluid medium with density ρ_f and viscosity μ_f as,

$$Re = \frac{d_p \, \rho_f \, v_f}{\mu_f} \tag{9}$$

When the drag coefficient C_D in Eq. (6) is replaced by Eq. (8), settling velocity for a single spherical particle in quiescent fluid becomes

$$v_f = \frac{g d_p^{\,2} \left(\rho_p - \rho_f\right)}{18 \mu_f} \tag{10}$$

It must be emphasized that Stokes's drag coefficient is only applicable at very low velocities and valid for values of Reynolds number less than about 1. This limit for Stokes flow corresponds to viscous dominant settling velocity.

At larger values of the Reynolds number, the inertial terms exercise an increasing influence on the flow dynamics. From the literature, the drag coefficients for the spherical particle submerged in the fluid are as follows:

$$C_D \approx \frac{18.5}{Re^{0.6}} \quad \text{for } 1 \le Re < 10^3 \text{ (intermediate flow regime)}$$

$$C_D \approx 0.44 \quad \text{for } 10^3 \le Re < 10^5 \text{ (Newton's flow regime)} \tag{11}$$

The study of settling phenomena has been performed by a considerable diversity of approaches. The literature information (Oliver, 1961) has suggested that the motion of a typical single particle should be influenced by both the motion and the presence of the other particles. The main effect of the motion of the other particles is to cause a return flow of liquid, while the presence of the other particles produced an effect similar to an increase in the viscosity of the dispersing liquid. In the literature correlations, the velocity for flow past a single sphere was used in order to obtain an equation relating the settling velocity of a suspension of mono-size spherical particles to the volume concentration of the solid phase.

Table 4 shows various literature correlations for relative settling velocity V_r in terms of solid volume concentration, *c*. Relative settling velocity V_r is defined as

$$V_r = \frac{v_s}{v_f} \tag{12}$$

In Eq. (12), v_s is settling velocity in a multi-particle system, and v_f is settling velocity for a single particle in a fluid.

The downward motion of the particles must cause an upward flow of liquid, and the velocity of this flow averaged for the whole flow cross-section of the tank must be the liquid fraction (1 - *c*) times the solid settling velocity of particles allowing only for return flow of liquid when *c* is defined as the solid volume fraction of the suspended fluid. In addition, the presence of other particles also impedes the motion of a typical particle in the same way as if there were an increase in the viscosity of the liquid, so that the

effective relative viscosity would reduce the settling rate of the suspended particles. Thus, the updated literature correlations [4] for settling velocity within a dilute solution were formulated considering these two factors.

$$v_s = v_f f_1(c) f_2(c) \tag{13}$$

In Eq. (13) f_1 and f_2 are empirical functions associated with a return flow effect due to the falling of the particles and a hindering effect of the particle precipitation due to the increased effective viscosity, respectively. These two functions were assumed to be dependent only on the solid volume fraction of suspension, *c*.

Figure 6 shows single free-fall velocities and multi-particle settling velocities as function of solid particle diameters. The calculations were performed by using a Stokes's flow approach (Eq. (10)) and the literature correlation for the settling rate of mono-sized spherical particles.

Typical literature correlations for relative settling velocity are shown in Table 4 to examine the interference or hindering effects of particle settling due to presence of the other particles for the range of solid particle concentrations. The results shown in the literature indicate that settling velocities of particles in a multi-particle system are different depending on the particle shape and solid concentration. The settling velocity of spherical particles was estimated under different solid contents in a slurry. In this case the Oliver (1961) correlation was used to capture the hindering effect of particle settling in a multi-particle system. Specific information on the waste simulant important for the present work is that the insoluble solids have particle sizes from 10 to 60 microns with a concentration of 25 wt%, a slurry density of 2495 kg/m^3, a slurry viscosity of 2 x 10^{-3} Pa-s. Volume concentration of particles in the continuous fluid phase is one of the key parameters associated with flow pattern and slurry characteristics. Weight fraction W for solids can be converted to volume concentration C for given densities of the fluid and solid phases.

$$C_v = 1 - \left\{ \frac{\left(\frac{\rho_f}{\rho_s}\right)}{\left(\frac{1}{W} - 1\right)} + 1 \right\}^{-1} \tag{14}$$

where ρ_f and ρ_s are the densities of fluid and solid, respectively.

From Eq. (14) volume fractions of CST solids (C_v) can be calculated as about 0.12 for the present operating conditions when their weight fractions in a slurry flow are 0.25. The results for settling velocity of the sludge particle are summarized in Table 5.

Table 4. Literature correlations for relative settling velocities based on solid volume fraction as stated in Ref. 4 (relative settling velocity V_r is defined by Eq. (12)).

Authors (Year)	Relative settling velocity correlations	Approach method
Burgers (1942)	$V_r = \{1+(\lambda_1+\lambda_2)c\}^{-1}, \lambda_1 = 15/8, \lambda_2 = 5$	Theoretical work
Steinour (1944)	$V_r = (1-c)^2 10^{-1.82c}$	Empirical work
Hawksley (1951)	$V_r = (1-c)^2\ exp\left\{-\frac{2.5c}{(1-0.609c)}\right\}$	Empirical work
Oliver (1961)	$V_r = \left(1-0.75c^{1/3}\right)(1-2.15c)$	Theoretical and empirical work

Table 5. Settling velocity and average settling times for different sludge particle sizes in slurries containing two different solid contents.

Particle size (microns)	Settling velocity (in/sec)			Average settling time (min.)*		
	0 vol% soilds	5 vol% solids	12 vol% solids	0 vol% soilds	5 vol% solids	12 vol% solids
5	0.00080	0.00052	0.00038	105	1,622	2,245
10	0.0032	0.0021	0.0015	263	401	561
20	0.0128	0.0083	0.0060	66	102	140
30	0.0289	0.0187	0.0135	29	45	62
40	0.0514	0.0332	0.0240	16	25	35
50	0.0803	0.0519	0.0375	11	16	23
60	0.116	0.0747	0.0541	7	11	16

Note:* Average time for solid particle to travel 50-in distance down to the tank floor under a slurry fluid containing a given amount of solid contents

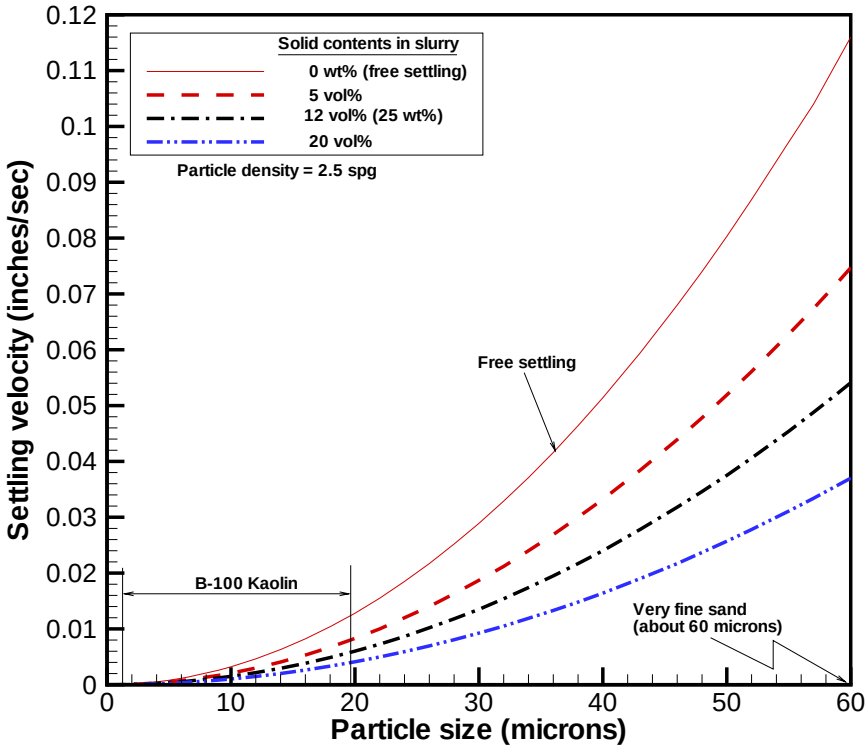

Figure 6. Particle settling velocity as function of particle sizes for different solid contents in a slurry

2.3 Incipient Erosion Velocity

When liquid flow passes over a stationary cohesive sludge heel containing solid particles, the flowing liquid is responsible for hydrodynamic forces being exerted on the individual particle of the sludge. In this case the initial movement of the top layer of the sludge is called critical or incipient condition of erosion. The degree of erosion resistance for a given particle size to the hydrodynamic forces of flowing fluid depends on the cohesion and adhesion forces. In this case, a further increase in the fluid momentum causes an increase in the magnitude of hydrodynamic forces. Hence, for a particular stationary sludge heel, a condition is eventually reached at which particles in the movable bed are not able to resist the hydrodynamic forces and, thus, solids of a given size resting in the top layer start to be eroded.

The present case to estimate the incipient minimum erosion velocity considers a stationary bed consisting of cohesive solid particles of uniform size, and liquid flowing over it. The literature data show that large particles are more easily eroded by streams than smaller ones. This phenomenon becomes more pronounced with small particles since the cohesion forces existing between the particles increase as the latter decrease in size. Dallavalle (1948) cited the equation for the incipient velocity of silting erosion

$$v_{ec} = \frac{0.00656}{d_p} \quad (15)$$

where v_{ec} is the incipient eroding velocity in ft/sec, and d_p the diameter of the particles in mm. Incipient erosion velocities provided by Eq. (15) are applicable to silting material, which contains small sizes of particles ranging from 5 (larger than clay) to 50 microns (close to very fine sand) in diameter.

The literature data [6] for the incipient erosion velocity are shown in Fig. 7. As can be seen in the figure, there exists for each grain size a certain velocity below which it will experience sedimentation, while above a certain velocity, called critical scour velocity, it will be eroded. Fluid velocity between these two velocities will suspend or transport solids for each solid size. The results show that the current velocity 2.27 ft/sec will erode the sludge layer for the particle sizes larger than clay material (about 5 microns). It should be emphasized that the incipient velocity of erosion is actually dependent on the critical shear stress at which incipient sediment begins to move. The critical shear stress of actual cohesive materials contained in Tank 5 depends on the composition of the different sludge material, the particle-size distribution, the particles' shape, and the packing.

Table 6 demonstrates reasonable agreement between the approximate analysis described above and the present velocity criterion used for the erosion and removal operations of Tank 5. Minimum fluid velocity for eroding the sludge of Tank 5 in Savannah River Site (SRS) has been established as 2.27 ft/sec for the analysis [6]. Thus, local fluid velocity at any distance from the nozzle is employed as a measure of the slurrying and mixing efficiency of the pump in Tank 5.

Table 6. Critical eroding velocities of particle pickup and removal for the various particle sizes

Particle size (microns) [class of particles]	Minimum velocity required to erode the sludge heel composed of uniform sizes of solids (ft/sec) [13]	Minimum erosion velocity criterion established by the previous work [6]
1 [clay]	6.562	2.27 ft/sec (for sludge removal)
5 [silt]	1.312	
50 [very fine sand]	0.131	
100 [fine sand]	0.066	

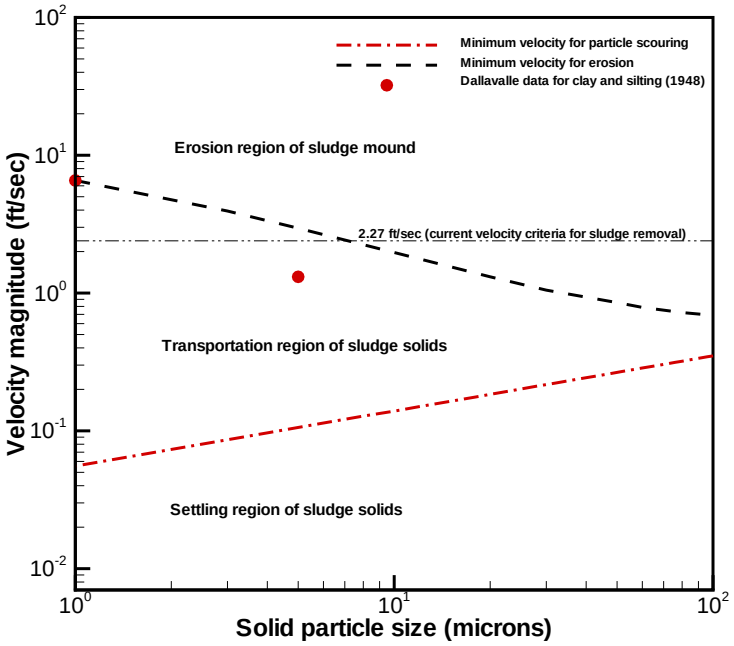

Figure 7. Velocity criteria for deposition, scouring, and erosion of sludge solids for the present operating conditions [6]

2.4 Tank 5 Model and Assumptions

From the previous discussions, the minimum suspension velocity required to lift sludge from the cohesive sludge heel was established to be 2.27 ft/sec. This value is consistent with the experimental observations in Tank 18 [5]. Therefore, the present work will use this velocity as the flow criterion in providing a recommended operational plan and strategy for sludge heel removal in Tank 5. The 2.27 ft/sec velocity will also be used to estimate the effective cleaning distance of SMP in the tank.

Tank 5 is cylindrical, 75 ft in diameter, and 24.5 ft high. For the nominal reference conditions shown in Table 2, the tank liquid level was kept 101 in. The tank has two 305 hp slurry pumps available to suspend and remove the sludge. Each pump has two horizontal discharge nozzles, each 4.4 in diameter. A total discharge flowrate of 7602 gpm corresponds to one of the nominal operating conditions shown in Table 2. There is a single suction at the bottom of the pump as shown in Fig. 2. The mixer is located about 16.5 ft away from the tank wall and about 24 in above the tank bottom as shown in Fig. 4. The modeling domain contains the internal flow obstructions representing twelve concrete columns to support tank structure and major pipes. Detailed flow obstructions modeled for the analysis are shown in Fig. 4. Detailed dimensions and pump layouts as modeled in the present work are illustrated in the figure. The model is a full three-dimensional representation of the entire tank to capture significant phenomena related to the turbulent behavior of the jet flow generated by the two pumps. For instance, flow obstructions such as cooling coil pipe clusters and valve housing distribution pipes

internal to the tank are simplified to maintain the same flow areas as prototypic geometry for computational efficiency. The graphical illustrations are presented in Figs. 8 and 9.

Detailed geometrical dimensions and operating conditions are provided in Table 2. Based on nozzle diameter and water properties, flow near the nozzle is fully turbulent since the Reynolds number for the reference operating conditions is about 2.7×10^6. The flow for the entire computational domain is assumed to be turbulent to give a reasonable representation of the liquid jet leaving the pump nozzle.

As discussed previously, the standard $k-\varepsilon$ model was used for the turbulence calculations. A three-dimensional model was run in steady-state and transient modes for the operating conditions of Tank 5 as provided in Table 2. Geometrical configurations and layout for the model are illustrated in Fig. 4. The calculations were performed for a fixed position of the jet nozzle when a steady-state mixing flow pattern in the tank was established. In addition, transient flow models were also run in $\pm 200^o$ oscillating mode with 1/3 rpm rotating speed to estimate mixing efficiency in terms of solid suspension capability due to fluid motion. The calculations consisted of several different cases to simulate various operating conditions for Tank 5 and to examine the sensitivities of the operating parameters with respect to the efficiency of sludge mixing.

The three-dimensional model was run in a steady-state mode for the fixed pumps to allow the jet flow to develop a flow pattern. For instance, when two pumps are used for the present Tank 5 model, the pumps are in a fixed orientation to maximize flow streams aimed at the sludge heel located near the corner of the tank. Both discharge jets are located at a horizontal plane 24 in above the tank floor. For the modeling analysis, total pump flowrate was 7602 gpm for the reference conditions and different pump flowrates for the sensitivity studies.

Figure 10 shows three-dimensional geometrical configurations as modeled in the CFD environment for the multi-pump simulations including the internal flow obstructions. For the simulations, a series of the modeling calculations will be performed in a fixed pump orientation until an optimized flow pattern near the potential location of the sludge heel is established. Physical model assumptions of the previous Tank 11 model [7] are used for the present calculations. Geometrical simplifications and physical model assumptions are listed as follows:

- There are no solid obstructions in the tank other than the pump support structure, 12 support columns, transfer pump and second SMP risers, nozzle housing, and valve housing distribution pipes as shown in Fig. 10.
- The pump nozzle for indexed operation is stationary, although in reality, the pump has a slight oscillation.
- The working liquid is water at $50\,^oC$.
- The liquid region is bounded by a free surface at constant atmospheric pressure.
- The model is isothermal. No energy equation is calculated.
- The flow in the entire model domain is assumed to be turbulent to give a reasonable representation of the liquid jet leaving the pump nozzle.
- The wavy motion of the free surface due to the interaction with the discharge jet is neglected. Literature data [6] show that the surface wave effect is negligible when

the ratio of liquid height above the nozzle to nozzle diameter is larger than 2.5. For a slurry mixer in Tank 5, the minimum ratio is about 230 for the 101-in liquid level case.

Three-dimensional numerical simulations are made for the Tank 5 modeling analysis. About 400,000 nodes for the three-dimensional computational domain shown in Fig. 10 have been established from the sensitivity studies of computational meshes. Figure 11 shows the computational meshes near the pump discharge plane.

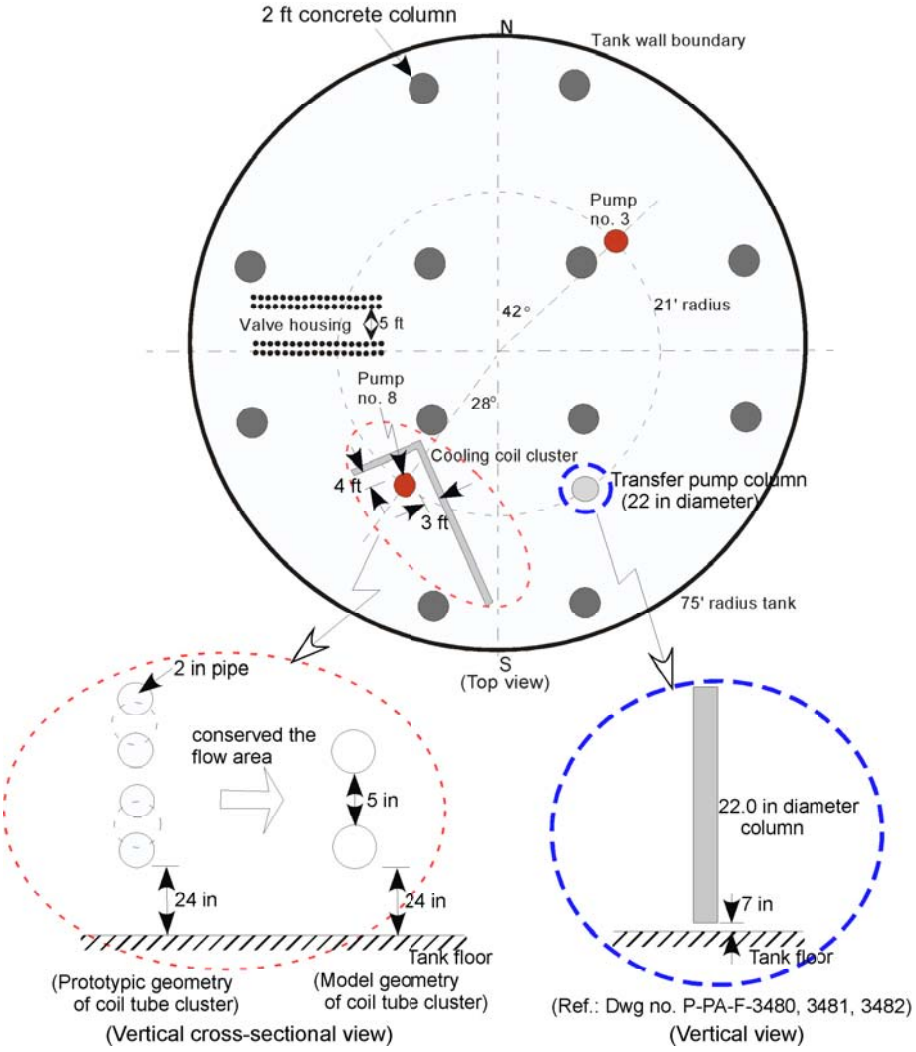

Figure 8. Tank 5 CFD model for the horizontal cooling coil pipe cluster near pump no. 8 and the transfer pump column (riser no. 6) inside Tank 5

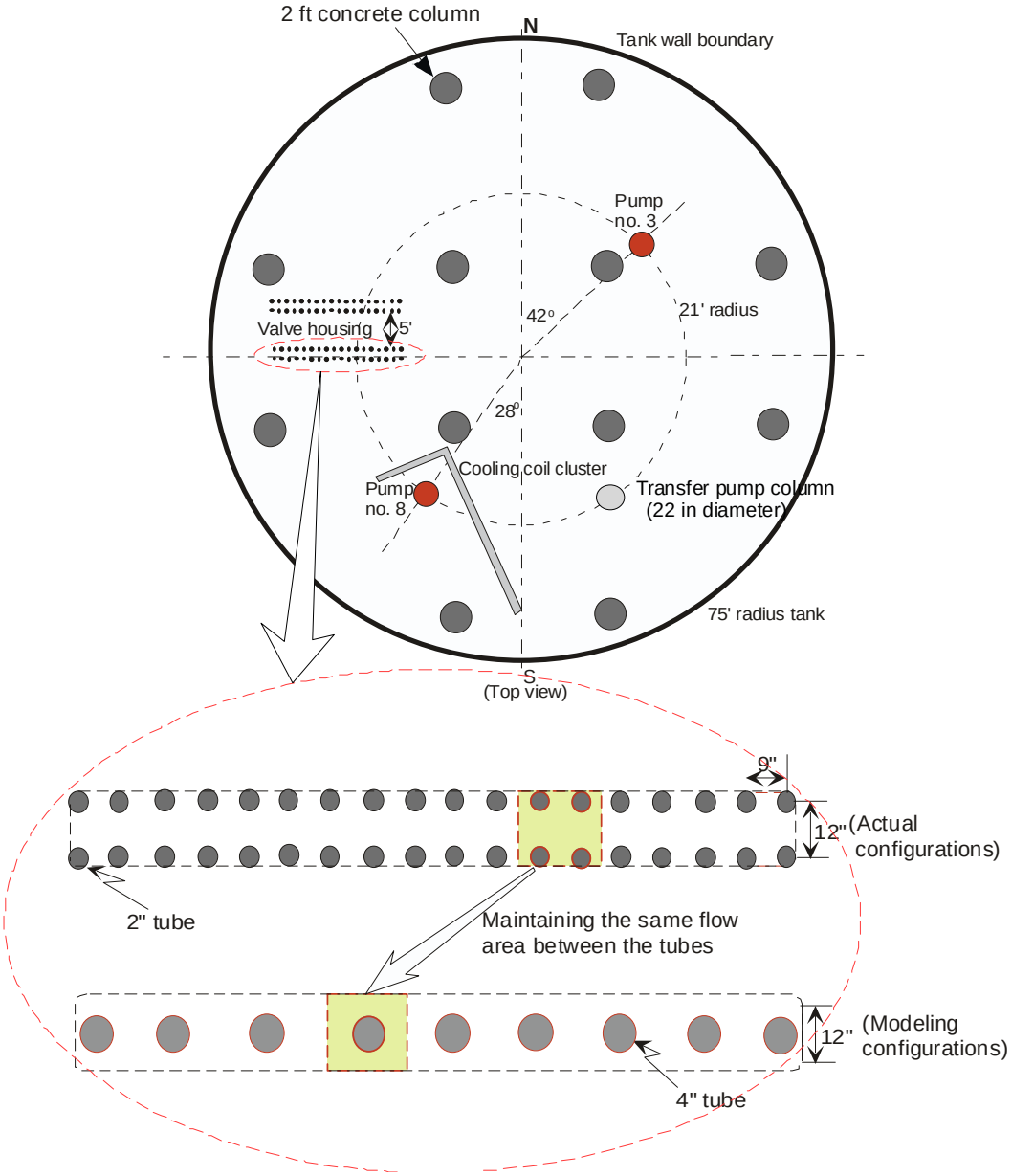

Figure 9. CFD model for the valve house distribution pipe on the three-dimensional computation domain of Tank 5

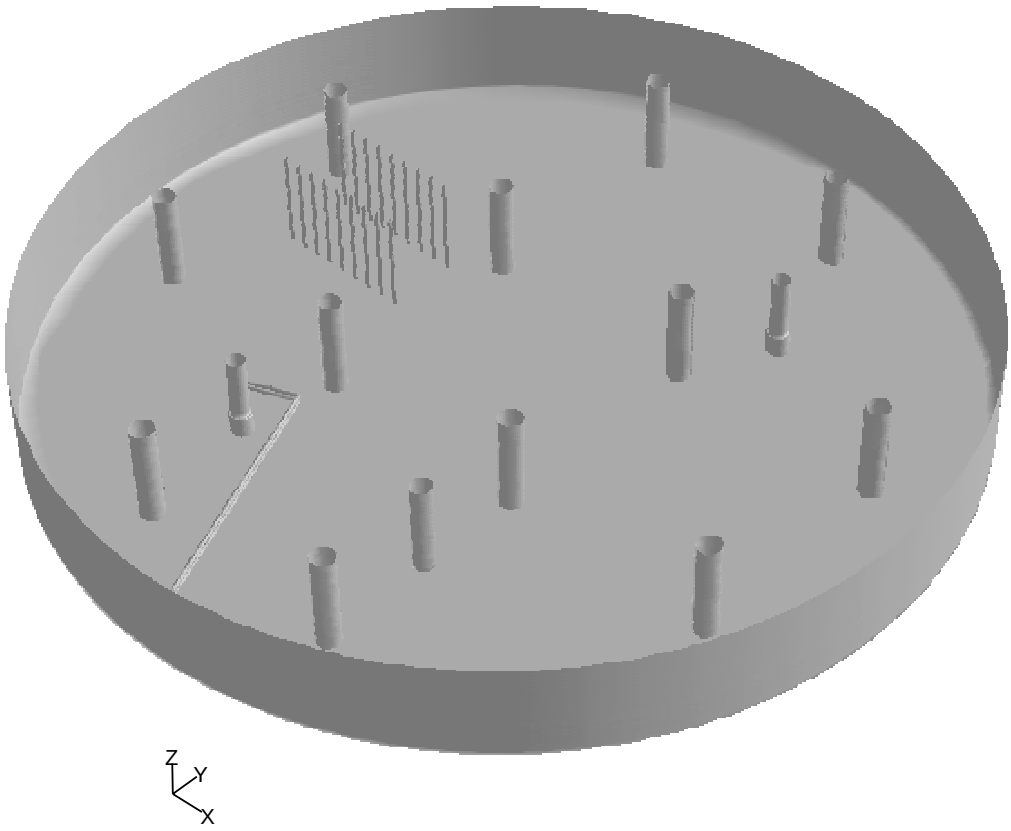

Figure 10. Three-dimensional computational domain as used in the Tank 5 CFD model

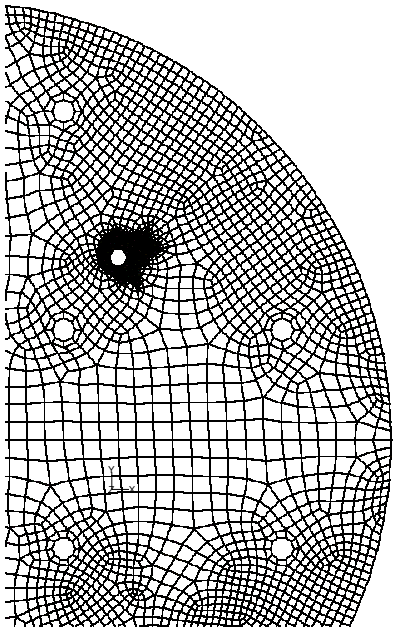

Figure 11. Computational meshes on two-dimensional plane near the pump as used in the calculations

3. Results and Discussions

A Tank 5 model has been developed by a CFD approach to include several internal flow obstructions such as twelve 2-ft support columns and major cooling coil distribution pipes in the computational domain and analyses performed to estimate circulation flow patterns within Tank 5 to evaluate the ability of the two slurry pumps to remove the sludge heel remaining in the tank. The mixing pumps are assumed to be stationary for ECR estimation of the pump. Oscillating operation mode was also considered for examining mixing performance for normal operating conditions. A flow velocity criterion is used as the primary indicator of the ability to erode cohesive sludge layer and to suspend sludge particles, based on the solution method established in the earlier discussions and the previous work [6].

The current model was simulated with the reference operating conditions as provided by the customer [2, 3], and it is mainly to evaluate flow circulation patterns and Effective Cleaning Radius (ECR) to develop an operational strategy for the sludge removal operations of Tank 5. The model was also used to perform sensitivity analyses for different tank levels, number of operating pumps, various pump operating modes such as indexed or rotating operations, pump flowrates, and different fluid properties. Reference design and operating conditions of Tank 5 used for the present analysis are provided in Table 2.

In Fig. 4, a potential sludge heel may be located near the west corner of the tank since it has the largest distance from the nearest pump and it has more flow obstructions than any other area does. This sludge heel is also based on the past experience of Tank 7

and Tank 8. Because of the distance from the nearest slurry pump to the sludge heel, as well as the apparent obstruction to the slurry jet flow formed by the concrete support columns and cooling coil distribution piping, major questions are the optimum number of operating pumps and the most effective discharge direction of each pump to remove the sludge heel. As shown in Fig. 4, Tank 5 has the cooling coil pipe cluster near the nozzle exit of pump no. 8.

The Tank 5 model with the reference conditions of Table 2 was used to estimate the distance at which the sludge removal velocity was maintained for two pump operations. The two pumps are pump no. 3 and no. 8, and they are stationary or oscillatory. The present calculations used 2.27 ft/sec as the minimum velocity for the sludge removal, which was estimated earlier using the previous works [4, 6, and 9]. The modeling results showed that when the sludge heel is assumed to be near the valve housing distribution piping at the west corner of Tank 5, the most ineffective pump orientation is the one with two pump nozzles opposing each other as shown in Fig. 12 because high dissipation of fluid momentum occurs near the center of the tank as result of direct fluid interactions. The most efficient orientations of the two pumps under indexed operating mode are presented in Fig. 13. The flow patterns corresponding to these two cases are compared in Fig. 14. As shown in the figure, the most efficiently indexed orientations of the two pumps have the large red area larger than minimum erosion velocity 2.27 ft/sec at the west corner of the tank, but the other has large blue area of near-zero fluid motion at the valve housing distribution piping region of the western tank corner.

As shown in Fig. 4, the present modeling domain includes 2-in cooling pipe cluster near the nozzle exit of pump no. 8. The results showed that the impact of the 2-in pipe flow obstructions on the pump ECR is found to be negligibly small as compared in Fig. 15. As shown in Figs. 16 and 17, flow patterns for the vertical plane crossing the nozzle exit are compared between the two cases without and with cooling coil pipe clusters near the pump nozzle exit. This is mainly due to the smaller pipe size, compared to the domain size of jet mixing area in the stagnant fluid medium as shown in Fig. 18. Figure 19 compares the degree of fluid rotations along the principal discharge direction of the pump for the two cases. Figure 20 compares local velocity magnitudes along the principal discharge direction of pump no. 8 between the flow obstruction results with and without cooling coil pipes including the free jet results without any flow obstructions. Table 7 compares quantitative magnitudes of the pump ECR under indexed two-pump run.

It is important to examine maximum cleaning distances for number of operating pumps and aiming directions of pump nozzle for efficient sludge removal operations of Tank 5. The modeling results showed that when there are flow obstructions on the far downstream side of the principal discharge direction, two pump run is more efficient that one pump run in terms of ECR since axial fluid momentum dissipation of pump nozzle no. 8 due to the presence of solid obstructions is recovered by the jetted flow of pump no. 3.

Figure 21 shows pictorial and quantitative comparisons of flow patterns between the two cases showing that the red region in the figure indicates the zone larger than suspension velocity of 0.6918 m/sec (2.27 ft/sec). When there is no solid obstruction along the principal discharge direction of the indexed pump nozzle as shown in Fig. 22, one pump run has larger ECR than two pump run does. Figure 22a shows three-dimensional region of potential sludge erosion for one pump run with the most efficient aiming angle of $\theta = 78^{o}$ (as shown in the same figure) under the indexed mode operations. The red

zone in the figure indicates the flow region larger than the minimum erosion velocity magnitude of 2.27 ft/sec. Figure 23 shows quantitative comparison of ECR's between one pump run with aiming angle of $\theta = 78^o$ and two pump run with aiming angles of $\theta = 78^o$ and $\zeta = 88^o$ under the indexed mode run. The results are summarized in Table 8. As compared in the figures, it is noted that the two pump run is more efficient than the one-pump run in removing the sludge located adjacent to the tank wall when flow obstructions such as support columns are present in the principal discharge direction of pump nozzle.

Table 7. Comparison of the modeling results for two different cases in the Tank 5 model in terms of maximum clearing distance (or ECR) under two-pump run as shown in Fig. 20

Cases	Pump position (Liquid level)	Presence of 2-in pipe obstructions near the pump nozzle exit	Nozzle velocity (ft/sec)	ECR* (2.27 ft/sec or 0.69 m/sec)
Tank 5 Model	Fixed (or indexed) (101 in)	no	80.2	39 ft
		yes	80.2	39 ft

Note: * ECR was defined as the maximum distance from the nozzle exit of the pump to the point at which local velocity reaches minimum suspension (or specified) velocity.

Table 8. Comparison of the ECR results for two different cases in the Tank 5 model under indexed pump operation

Cases	Pump position (Liquid level)	Number of operating pumps	Aiming directions of pump nozzle	Nozzle velocity (ft/sec)	ECR* (2.27 ft/sec or 0.69 m/sec)
Tank 5 Model	Fixed (or indexed) (101 in)	One pump run**	See Fig. 21+	80.2	35 ft
			See Fig. 23++	80.2	41 ft
		Two pump run**	See Fig. 21+	80.2	39 ft
			See Fig. 23++	80.2	37 ft

Note: * ECR was defined as the maximum distance from the nozzle exit of the pump to the point at which local velocity reaches minimum suspension (or specified) velocity.

** ECR variation depending on nozzle aiming directions

+ For major flow obstruction present in the principal discharge direction of pump no. 8

++ For no major flow obstruction in the principal discharge direction of pump no. 8

Flow patterns were evaluated for three different tank levels with all other parameters fixed. The reference tank level was 101 in as shown in Table 2. Lower tank levels of 45 in and 70 in were selected for the sensitivity analysis of tank level. When two pump nozzles of no. 3 and no. 8 are aiming at the western corner of the tank near the valve housing distribution piping area, Figure 24 compares flow contour plots at the nozzle exit plane of 24 in above tank floor among the three different tank levels. Flow patterns at the corner region adjacent to the valve housing piping area are more active than in the central region of the tank because of combined fluid vortices generated by the two pumps. In Fig. 25 flow velocities along the principal discharge direction of the pump no. 8 exit plane for the two-pump indexed operation are quantitatively compared between the three liquid levels. In the figure maximum ECR for the reference tank level (101 in) are found to be about 10% higher than the lowest tank level of 45 in. The results for the 101 in and 70 in tank levels show negligible difference in the pump ECR predictions as shown in Table 9. The sensitivity results show that the lower tank level case has higher dissipation of fluid momentum than the other case since turbulent dissipation rate increases along the discharge direction as tank level decreases. These results are consistent with the previous modeling results [5 - 8] and operational experience of Tank 18 [6]. Quantitative comparison for the three different tank levels of Tank 5 is made in terms of maximum cleaning distance as shown in Table 9.

Table 9. Sensitivity results for different tank levels in the Tank 5 model under the reference operating conditions except for tank level in terms of maximum clearing distance (or ECR)

Model	Tank liquid level	Pump elevation from tank bottom	Nozzle exit velocity (ft/sec)	ECR* (2.27 ft/sec or 0.69 m/sec)
Tank 5 Model	101 in**	24 in**	80.2**	39 ft
	70 in	24 in**	80.2**	39 ft
	45 in	24 in**	80.2**	35 ft

Note: * ECR was defined as the maximum distance from the nozzle exit of the pump to the point at which local velocity reaches minimum suspension (or specified) velocity of 2.27 ft/sec.
** Reference operating conditions defined in Table 2.

Rotational effects on jet dissipation were also examined. According to the operating plan of Tank 5 pump [1, 2], the pump will oscillate at $\pm 200^{o}$ rotation with about 1/3 rpm rotating speed. For the numerical simluations, the transient behavior was simulated in a discrete way. Each rotating step had 20^{o} increment at a time interval of 10 seconds, and the rotating direction was changed every 100 seconds, resulting in $\pm 200^{o}$ oscillation with 1/3 rpm rotating speed. As shown in Fig. 26, the modeling results show that one-dimensional ECR distance along the principal discharge direction of the nozzle exit plane for the indexed run is at least about 6% larger that the oscillating pump run under

two pump run. Quantitative ECR comparison for the operating modes is made in Fig. 27. However, as shown in Fig. 26, the oscillating pump case has flow velocities much larger than the stationary pump for the region far away from the discharge direction and near the tank wall boundary. Thus, the zones larger than minimum velocity required for erosion at the nozzle exit plane are about the same for the two cases of indexed and oscillating pump operations.

When the reference tank level was 101 in as shown in Table 2, and the two cases kept all other parameters fixed except for pump operating mode, Table 10 shows quantitative comparison of sludge removal capabilities in terms of maximum cleaning distance. The clearing distance is defined as the distance from the nozzle exit of the pump to the location reached to the minimum 2.27 ft/sec velocity of sludge removal. As shown in Fig. 28, the sensitivity results show that the model with oscillatory pump operation has higher radial dissipation of fluid momentum than the steady-state model with indexed pump run. The results in the figure are for both pump nozzles aiming at the center of Tank 5.

Effects of pump rotating direction for each of the two pumps on sludge mixing are studied under the reference conditions as defined in Table 2. Two cases are considered for this study. One is Case A with both pumps oscillating in the same direction. The other is Case B with each pump oscillating in the opposite direction. The simulation results show that Case A is better than Case B in terms of sludge suspension capability because Case B has larger local momentum dissipation as result of direct interactions, compared to Case A. Figure 29 shows two snapshots comparing quasi-steady flow pattern results of the two cases at two transient times of 190 and 210 seconds. Typical quasi-steady flow patterns for oscillating mode run of Case A are shown in Fig 30. The red region in the figure indicates the area which has local velocity larger than minimum velocity of 0.692 m/sec (2.27 ft/sec) required to erode sludge material. The results show that it takes about 3 minutes to reach quasi-steady flow patterns under Case A or Case-B operating condition.

Table 10. Sensitivity results for different pump operating modes in the Tank 5 model under the reference operating conditions except for pump operation mode in terms of maximum clearing distance (or ECR)

Cases	Pump operating mode	Pump elevation from tank bottom	Nozzle exit velocity (ft/sec)	ECR* (2.27 ft/sec or 0.69 m/sec)
Tank 5 Model	Indexed mode**	24 in**	80.2**	39 ft
	Oscillating mode	24 in**	80.2**	35 ft

Note: * ECR was defined as the maximum distance from the nozzle exit of the pump to the point at which local velocity reaches minimum suspension (or specified) velocity of 2.27 ft/sec.

** Reference operating conditions defined in Table 2.

As a strategy of sludge heel removal operations, there are indexed and oscillating operation modes. The indexed operation mode is for eroding cohesive sludge heel, and then the oscillating mode is followed for suspending and mixing the loosely settled sludge particles. In this case, it is desirable to predict mixing efficiency in association with the number of sludge removal batches necessary before the beginning of next sludge erosion cycle. In this case the mixing efficiency is defined as the ratio of the area larger than minimum suspension velocity to total tank area at the pump nozzle exit plane. From the historical information, sludge particle size ranges from few microns up to maximum 100 microns. Although their average size is known as about 10 to 15 microns, the present analysis uses 60 microns, corresponding to fine sand size, for a conservative estimation of settling and suspension.

Settling time for 60-micron sludge particle is about 7 minutes for 0 wt% fluid and 16 minutes for 25 wt% as shown in Table 5. Minimum velocity required for suspending 2.5 spg sludge particle is about 0.38 ft/sec under 101 in tank level. Figure 31 presents quasi-steady flow patterns at the nozzle exit plane for $\pm 200^{o}$ oscillating mode with the same rotating direction (Case A) under two pump run. In the figure the red region indicates the zone larger than 0.116 m/sec (0.380 ft/sec) suspension velocity of 60 micron sludge particle as shown in Table 3. Quantitative estimations of local velocity magnitudes along the line A-B, corresponding to the velocity contour plots, are shown in Figure 32. The results in the figure show that settling time for the 60-micron particle allowable during 1/3 rpm oscillating pump operations is about 80 seconds, which is much smaller than the free settling time of 7 minutes. The numerical comparison is shown in Table 11. The exception is for the region within about 0.5 ft distance from the tank wall as indicated in Fig. 32. This means that the 1/3 rpm oscillating pump operations keep 60-micron sludge particles suspended except for the 0.5-ft wall boundary region. In this case mixing efficiency is found to be about 97% corresponding to the area ratio of the mixing area excluded 0.5-ft wall boundary region to total tank cross-sectional area.

Table 11. Comparison of settling times of 60-micron sludge particle between maximum settling time allowable during two pump operations and free settling velocity of quiescent fluid medium in Tank 5

Number of operating pumps	Nozzle exit velocity (ft/sec)	Max. allowable settling time* of 60-micron sludge during tank mixing with 1/3 rpm pump oscillations	Settling time# for a quiescent fluid medium containing 0 or 12 vol% sludge containing 60-micron solids in 50-in tank level	
			0 wt% sludge particles (0 vol.%)	25 wt% sludge particles (12 vol.%)
2	80.2	~ 80 sec.	7 min.	16 min.

Note:* Time duration to have fluid velocity lower than min. suspension velocity of 60-micron sludge particles
Settling time was estimated for 50-in traveling distance of a given particle size.

As discussed earlier, a flow velocity criterion has been used as the primary indicator to assess the sludge removal capability for different operating conditions. Flow patterns were evaluated for different pump flowrates with all other parameters used by the reference conditions. The reference pump speed is not determined yet. Different pump flowrates were used for the sensitivity runs, assuming that the nominal flowrate of 3801 gpm could increase up to 4156 gpm or may reduce down to 20 % lower flowrate of 3040 gpm if necessary. The results of flow velocity magnitudes along the principal discharge direction of the pump no. 8 exit plane are compared among three different pump flowrates under one pump run in Fig. 33. It is noted that the higher pump flowrate is generally more efficient than the lower in terms of sludge removal capability, but it is about the same near the center of the tank in terms of flow circulation patterns. Table 12 shows quantitative comparison of the calculated maximum ECR values among the three different flowrates per nozzle, 3040 gpm, 3801 gpm, and 4156 gpm, assuming that 3801 gpm is the baseline reference flowrate per nozzle as shown in Table 2. The results show that the effective cleaning distance increases by about 10 % with respect to the reference flowrate of 3801 gpm when pump flowrate increases from 3801 gpm to 4156 gpm.

Table 12. Sensitivity results for different pump flowrates in the Tank 5 model under the reference operating conditions except for pump flowrate in terms of maximum clearing distance (or ECR)

Cases	Flowrate per nozzle	Nozzle exit velocity (ft/sec)	Pump elevation from tank bottom	ECR* (2.27 ft/sec or 0.69 m/sec)
Tank 5 Model	3040 gpm	64.2	24 in**	31 ft
	3801 gpm**	80.2**	24 in**	41 ft
	4156 gpm	87.7	24 in**	45 ft

Note: * ECR was defined as the maximum distance from the nozzle exit of the pump to the point at which local velocity reaches minimum suspension (or specified) velocity of 2.27 ft/sec.
** Reference operating conditions defined in Table 2.

It is important to recognize that local velocity is not the only parameter affecting the ability of the liquid stream to suspend and transport sludge. The length of time that the sludge is exposed to the liquid stream is also important, and this effect was quantified in the previous analysis by using the empirical approach [7] since this effect is not captured in the present analysis. From the previous results for Tank 16 operations with 0.25 rpm of average rotational slurry pump [10], the pump operating time of about 500 hours was required to get cleaning radius of 37.5 feet. These data are applied to the present Tank 5 operations with fixed pump orientation since the CFD simulation results show that the steady-state cleaning distance covers the sludge area for the potential operating conditions. In this case, the main assumption was that material characteristics of Tank 5 sludge is similar to that of Tank 16 sludge.

The mixing time for the pump operation with the fixed pump orientation aiming at the sludge heel was estimated using the Tank 16 data [10]. From the present modeling

results, the jetted spread angle was found to be about 14^o as defined in Fig. 34. For the present operating conditions with indexed slurry pump, the pump operating time can be estimated by the equation. That is,

$$t = t_{tk16}(x)\left(\frac{\theta}{360}\right)N_n \qquad (7)$$

In Eq. (7) $t_{tk16}\ (x)$ is the pump operating time at the cleaning radius of x ft, which can be obtained from Tank 16 data [10]. The parameters, θ and N_n, are jet spread angle and number of discharge nozzles for each pump, respectively. When the current indexed operating condition of Tank 5 slurry pump is given as $\theta = 14^o$, and $t_{tk16}(x = 39\ ft) \approx 500$ hrs is provided to Eq. (7) by the previous data [10, 11], about 40 hours' pump operation time is required for each indexed pump orientation in order to suspend cohesive sludge materials. However, some sludge regions of Tank 5 are located less than about 35 ft away from each pump, well within the 35 ft ECR distance of the oscillating SMP operation mode. When two slurry pumps operate simultaneously in indexed or oscillating mode, only about 30% of the total area in the tank requires a cleaning radius of larger than 35 ft for the sludge removal. Based on these operating conditions, about 266 hours of total pump run time is required for sludge removal. Approximately 160 hours' of indexed runs are required for the remote sludge located at larger than 35 ft distance from the pump and 106 hours required for oscillating mode of operation for less than 35 ft distance.

The present analyses have been performed using 50^{o}C water as the working fluid for the nominal reference operating conditions. Different fluid properties, which are similar to typical slurry fluid in Tank 5 as provided by customer [2], were used to examine the sensitivity of the flow patterns to these changes. The results show that the flow patterns are not sensitive to changes of fluid properties. At the discharge plane, there are no apparent differences in flow evolution as shown in Fig. 35. In the figure local velocity magnitudes of water and potential slurry flows along the principal discharge direction of the pump no. 8 nozzle are compared between the two cases of one-pump and two-pump runs. At the 24 in elevation of the pump exit plane, slurry flow around the flow obstructions present on the principal discharge direction of the pump nozzle dies out slightly more quickly than water since radial viscous diffusion is increased relative to axial convection when the fluid viscosity is increased from water (1 cp) to slurry (2 cp). When there are no flow obstructions on the principal discharge direction of the pump nozzle, slurry ECR is a little bit larger than the water ECR as compared in Table 13. It is noted that the secondary radial flow induced by the slurry due to the presence of the flow obstructions is larger than that for water because of the increased diffusion in the momentum transport. When the maximum clearing distance (or ECR) is defined as the distance over which the jet velocity exceeds the minimum suspension velocity, ECR for water is about the same as that of slurry. This result is consistent with the previous results [5, 7].

Figure 36 can be used to predict the location of potential sludge heel and to estimate the amount of cohesive sludge in Tank 5 that is beyond the erosion capability of the slurry pump under the reference operating conditions. An engineering estimate is that sludge material would remain in the crosshatched region as shown in the figure. Assuming the sludge heel is cohesive, the volume of this region has been evaluated numerically and is approximately 3,100 gal as shown in Table 14. The calculation also assumed that sludge heel height for the crosshatched region in Fig. 36 remains the same as the initial height of ~11 inches [2] during pump operations and the 1-in thick cohesive sludge layer

remains near and below the horizontal cooling coils on the tank floor. In this calculation, volume of non-cohesive solid material precipitated on the tank floor is not considered. That is, the deposition of large particulates would be expected to follow behind the rotational motion of the jet, leaving an annular ring at the peripheral region near the tank wall. The particulate would remain there until the opposing jet is passed over that same region.

The modeling results demonstrate that lower tank level and lower pump flowrate, and higher pump elevation provide smaller cleaning capabilities with respect to the reference conditions. It is emphasized that the higher tank level is more efficient than the other in terms of sludge removal capability. This is consistent with the previous results [5, 6, and 8]. This information will assist in the sludge suspension and removal plans for Tank 5 operations.

Table 13. Sensitivity results for different fluid properties in the Tank 5 model in terms of maximum clearing distance (or ECR) under one-pump run of pump no. 8 and two-pump run of pump no. 3 and no. 8

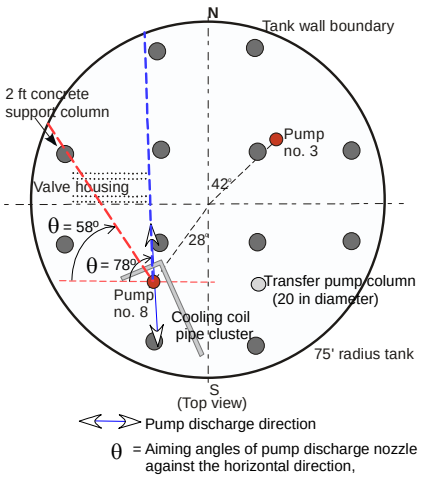

Cases	Pump operating mode, aiming angle of pump no. 8, (Liquid level)	Tank fluid	Nozzle velocity (ft/sec)	ECR* (2.27 ft/sec or 0.69 m/sec)
Tank 5 Model	Indexed one-pump run, $\theta = 78^{o}$ (no flow obstruction in the principal discharge dir.) (101 in)	Water	80.2	40.5 ft
		Potential slurry (1.2sg and 2cp)	80.2	40.8 ft
	Indexed two-pump run, $\theta = 58^{o}$ (flow obstruction present in the principal discharge dir.) (101 in)	Water	80.2	39.0 ft
		Potential slurry (1.2sg and 2cp)	80.2	38.4 ft

Note: * ECR was defined as the maximum distance from the nozzle exit of the pump to the point at which local velocity reaches minimum suspension (or specified) velocity.

The steady-state flow patterns on the horizontal discharge plane follow a series of parabolic curves similar to that of a free jet [14]. Vertical velocity profiles are changed from a bell-shaped curve near the exit of the nozzle to a near-uniform velocity near the tank wall boundary as shown in Fig. 3. These are in agreement with the previous results and the literature data [6].

When two pumps are operated aiming at the sludge heel located behind the support columns, pump operation with flow obstructions of the support columns (using pump no. 8) has better performance by about 15%, compared to one-pump run under the same operating conditions as graphically presented in Fig. 21. The results for flow velocities along the principal discharge line of Tank 5 crossing the flow obstruction are quantitatively compared between the two cases in the same figure. These results are mainly due to the combined flow effects generated by the secondary pump when the obstructions are present inside the flow field. It is noted that the presence of flow obstructions such as concrete support columns were advantageous for certain pump orientations in terms of guidance of the flow direction as shown in Fig. 22a. This is consistent with the previous modeling results [7].

As the modeling results discussed earlier, when fluid velocity is used as a scouring criterion to pick up and suspend cohesive sludge, flow fields induced by the slurry pump under the reference operating conditions as defined in Table 2 are adequate for the sludge removal operation of Tank 5. The exception is the west corner region within about 5 ft of the wall, which is located near the roof support columns as shown in Fig. 36, assuming the minimum velocity required to suspend waste sludge is 2.27 ft/sec. Maximum clearing distance of the slurry mixer for the reference operating conditions of one-pump indexed run is found to be about 41 ft for the pump orientation of no flow obstructions along the principal discharge direction. When flow obstructions are present in the nozzle direction, sludge removal domain of the cleaning distance of 39 ft under two pump run is illustrated in Fig. 36.

A series of sensitivity calculations has been performed to determine what operational conditions result in better cleaning capability of the sludge using the existing waste removal equipment.

Table 14. Volume predictions of the sludge remaining after the referenced sludge removal operations

Pump flowrate per nozzle	Tank level	ECR	Volume of the sludge heel*
3801 gpm	101 in	39 ft	about 3,100 gallons

Note: * Numerically calculated assuming that sludge heel height for the crosshatched region in Fig. 36 remains the same as the initial height of ~11 inches [2] during pump operations and the 1-in thick cohesive sludge layer remains near and below the horizontal cooling coils on the tank floor.

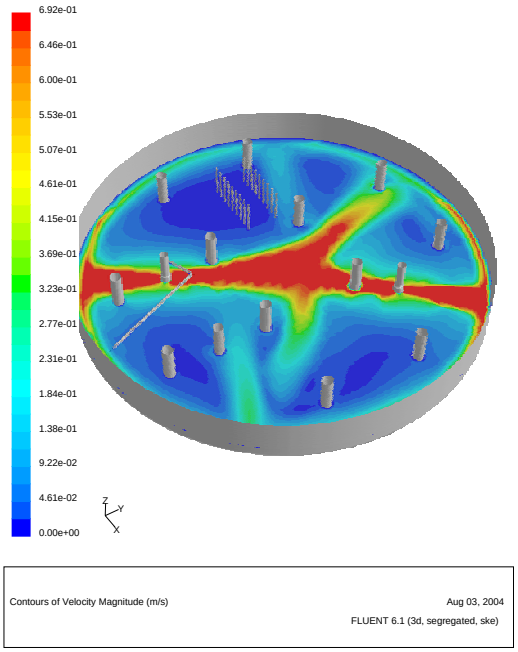

Figure 12. Flow patterns at the pump discharge plane for the inefficiently indexed pump orientations of two opposing pump operations showing that the red region indicates the zone larger than 0.6918 m/sec (2.27 ft/sec) suspension velocity

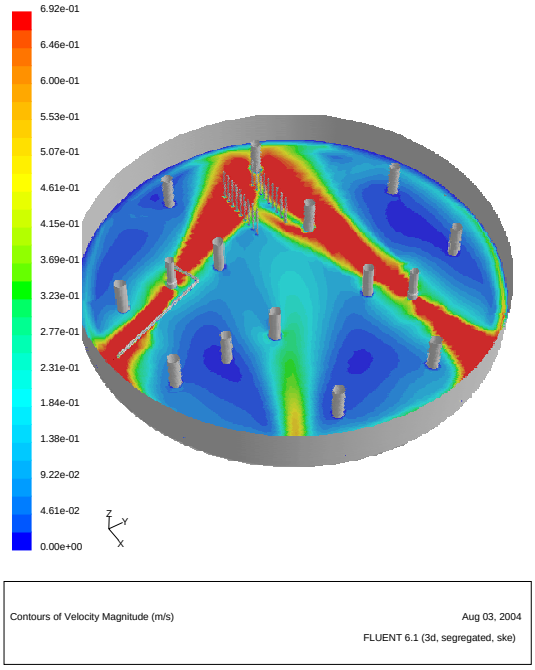

Figure 13. Efficient flow patterns at the pump discharge plane crossing the cooling coil tube for two-pump operation showing that the red region indicates the zone larger than 0.6918 m/sec (2.27 ft/sec) suspension velocity

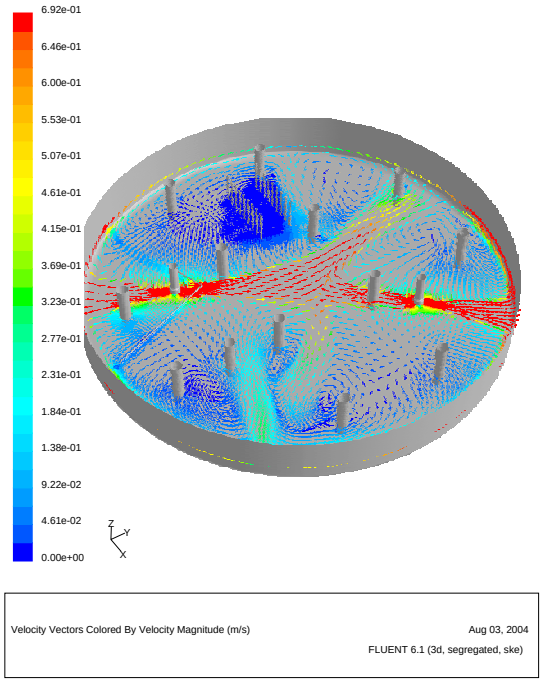

(Inefficiently indexed pump orientations)

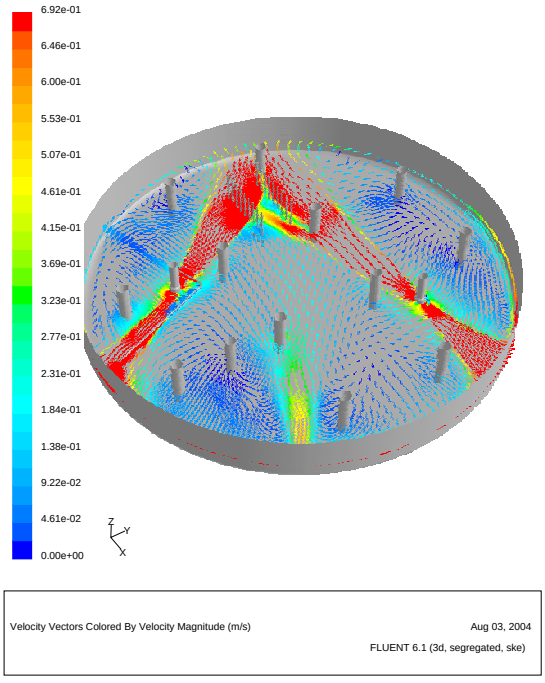

(Efficiently indexed pump orientations)

Figure 14. Comparison of two flow circulation patterns at the pump discharge plane crossing the cooling coil tube for two-pump indexed operation showing that the red vector indicates the one larger than 0.6918 m/sec velocity magnitude (2.27 ft/sec) required to erode sludge layer

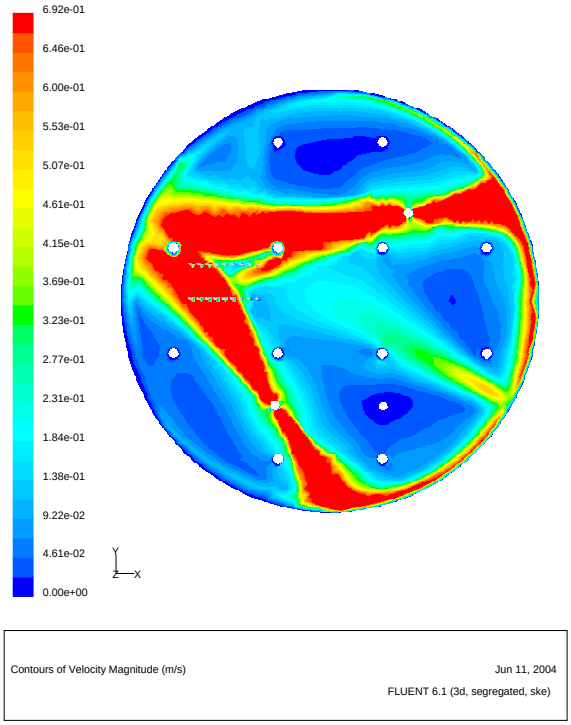

(Model with no flow obstruction near the nozzle exit of pump no. 8)

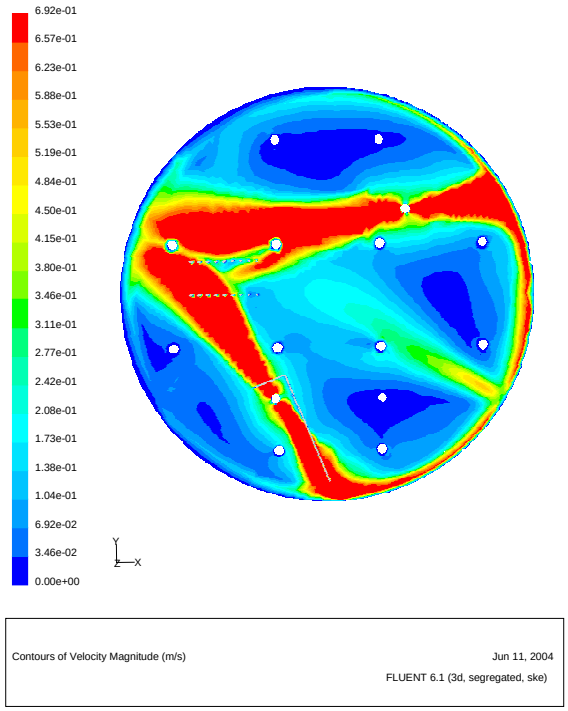

(Model with flow obstruction near the nozzle exit of pump no. 8)

Figure 15. Comparison of mixing zones at the horizontal nozzle exit plane between the models with and without cooling coil pipe clusters adjacent to pump no. 8

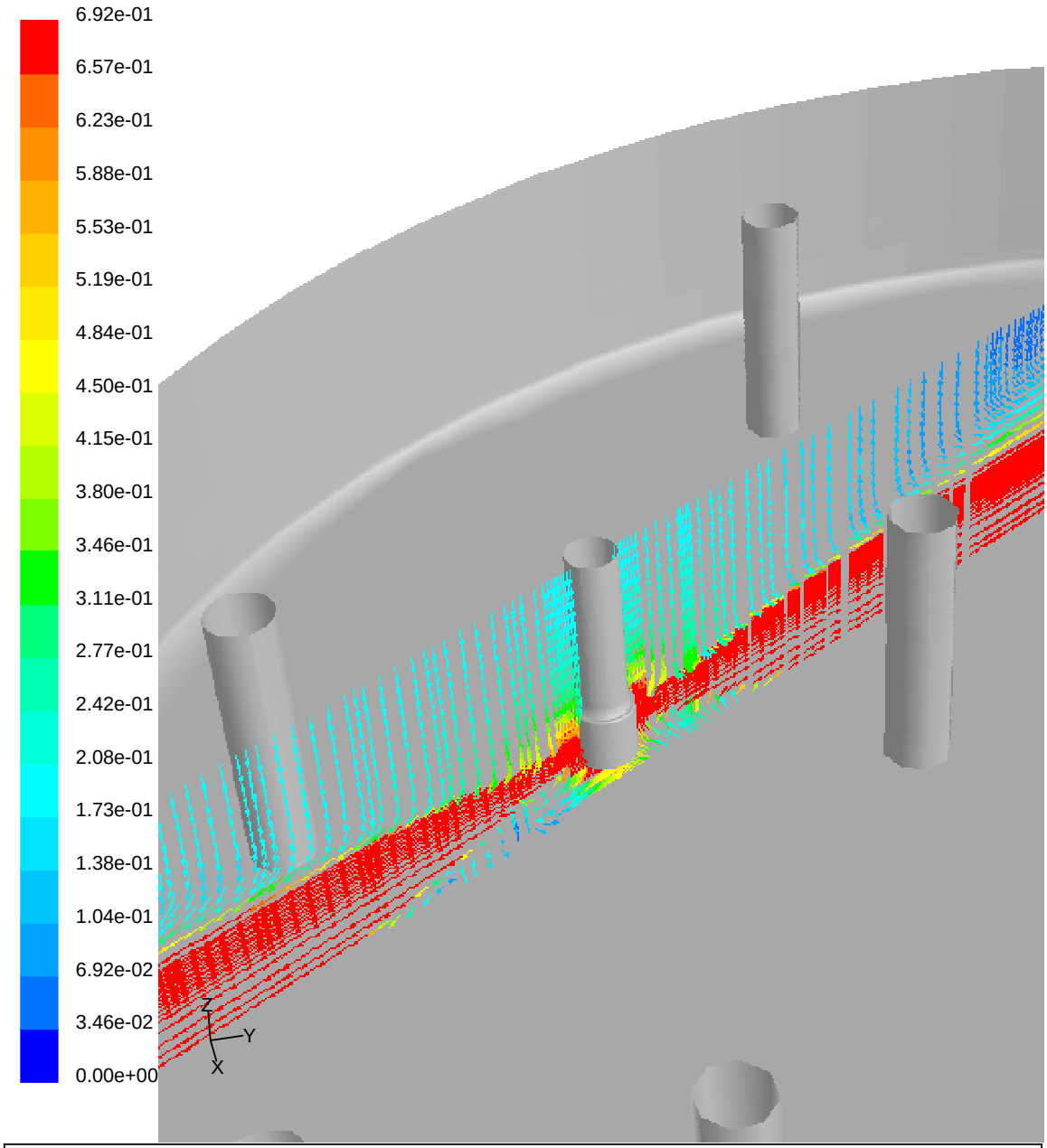

Figure 16. Flow patterns without cooling coil pipes showing that the red region indicates the zone larger than 0.6918 m/sec (2.27 ft/sec) suspension velocity

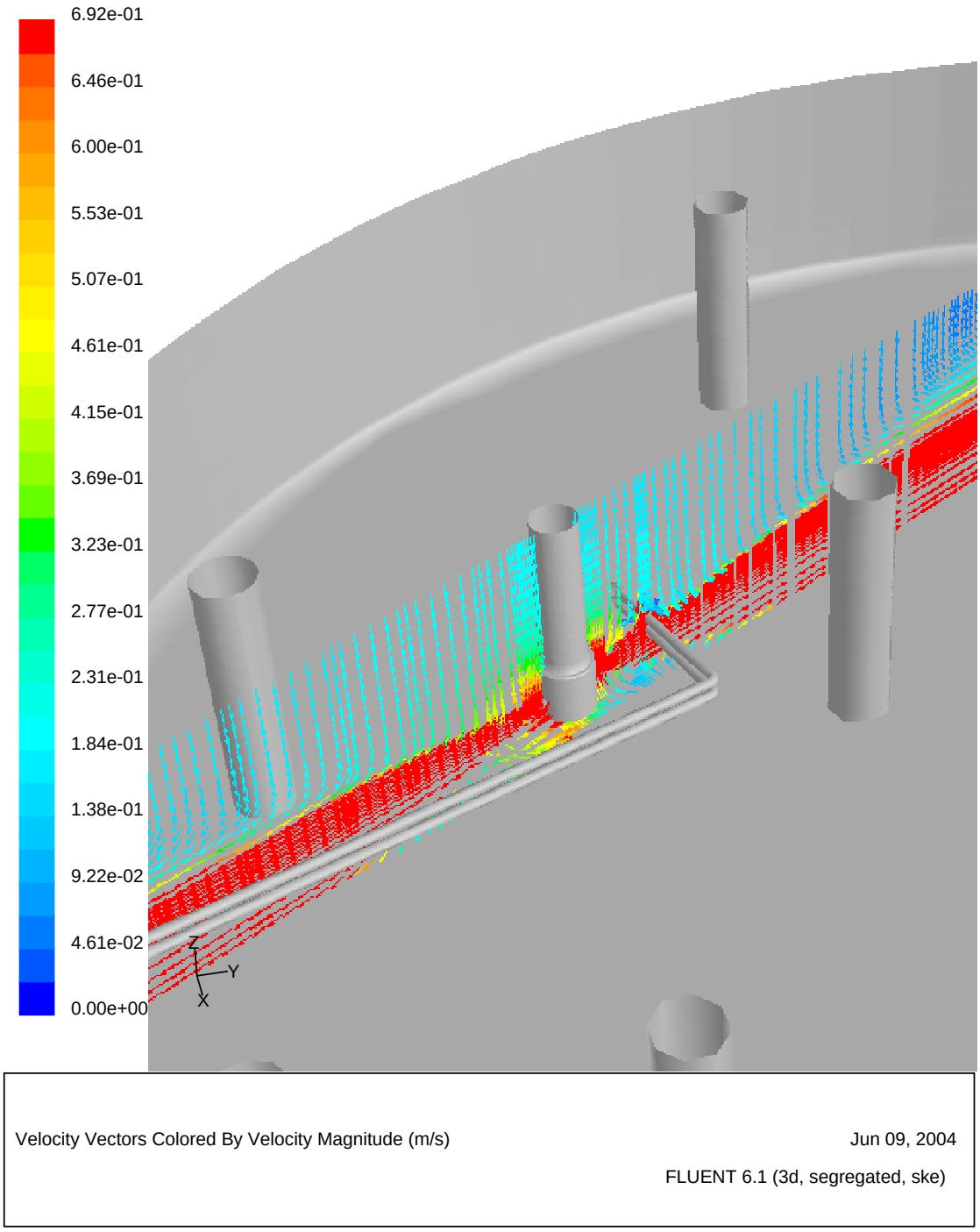

Figure 17. Flow patterns with cooling coil pipes showing that the red region indicates the zone larger than 0.6918 m/sec (2.27 ft/sec) suspension velocity

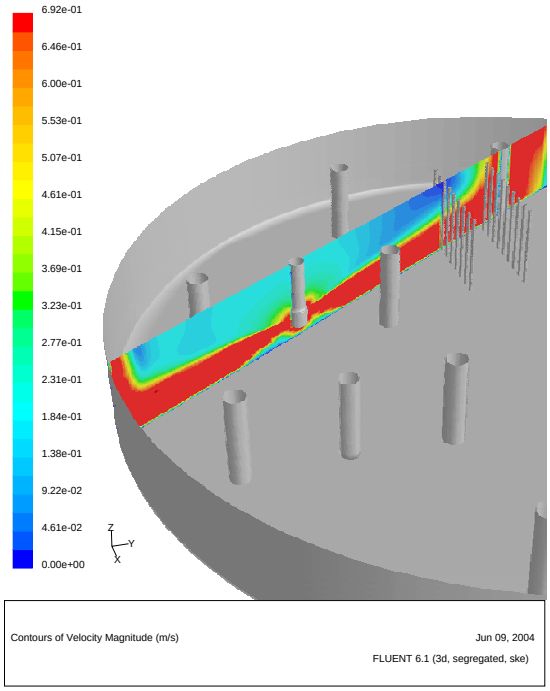

(Model with no flow obstruction near the nozzle exit of pump no. 8)

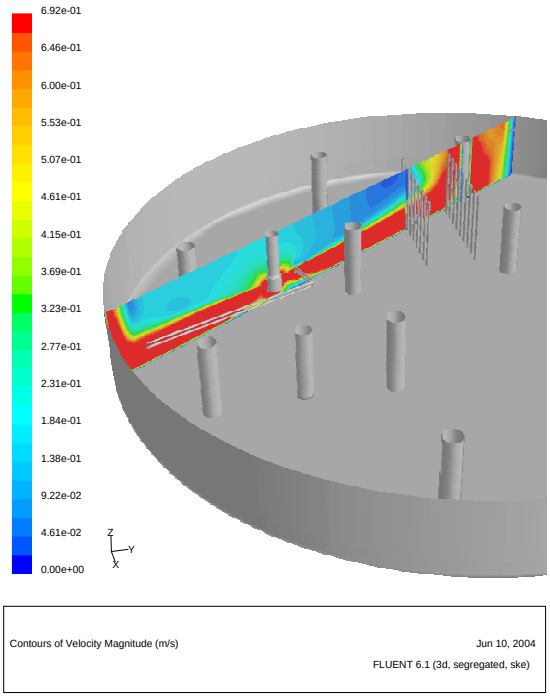

(Model with flow obstruction near the nozzle exit of pump no. 8)

Figure 18. Comparison of flow pattern results at the vertical nozzle exit plane between the cases without and with the presence of cooling coil pipes near the pump nozzle exit showing that the red region indicates the zone larger than 0.6918 m/sec (2.27 ft/sec) suspension velocity

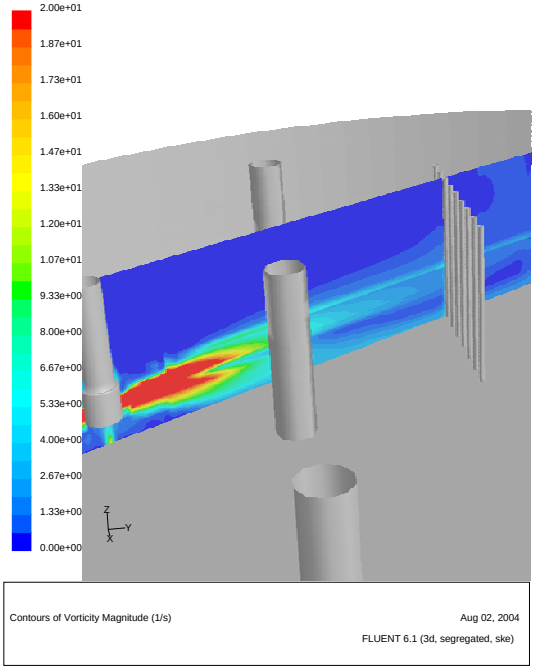

(Case with no cooling coil pipe cluster neat pump exit)

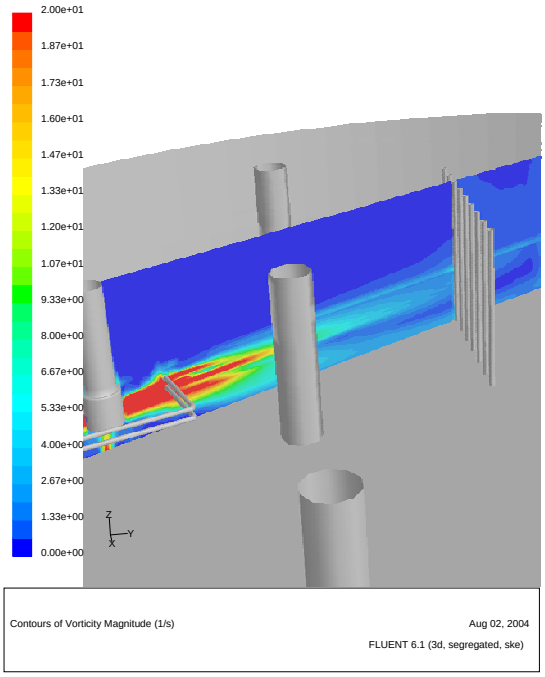

(Case with cooling coil pipe cluster neat pump exit)

Figure 19. Comparison of degree of fluid rotations near the vertical nozzle exit plane between the cases without and with the presence of cooling coil pipes near the pump nozzle exit showing that the red region indicates the zone larger than 0.6918 m/sec (2.27 ft/sec) suspension velocity

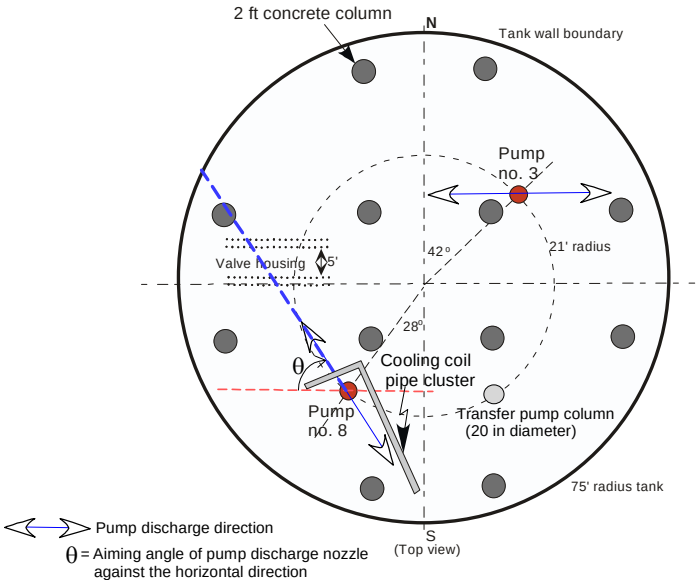

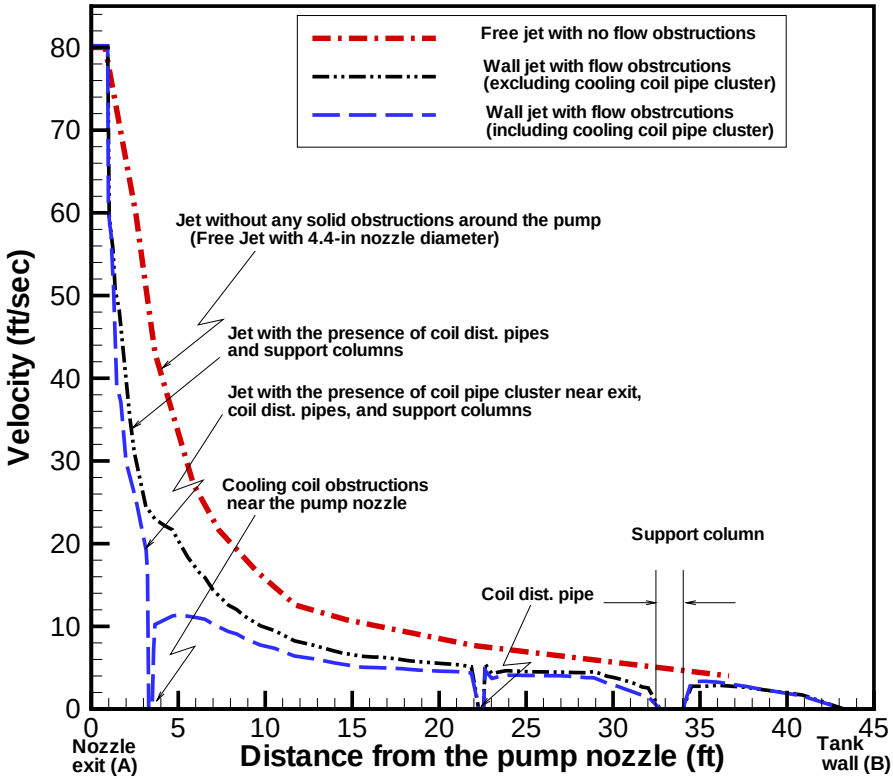

Figure 20. Quantitative comparison of velocity magnitudes between the free jet results without any flow obstructions and the wall jet results with and without cooling coil pipes along the principal discharge line A-B of pump no. 8 (The wall jet cases are for two-pump indexed operation ($\theta = 58^{o}$).)

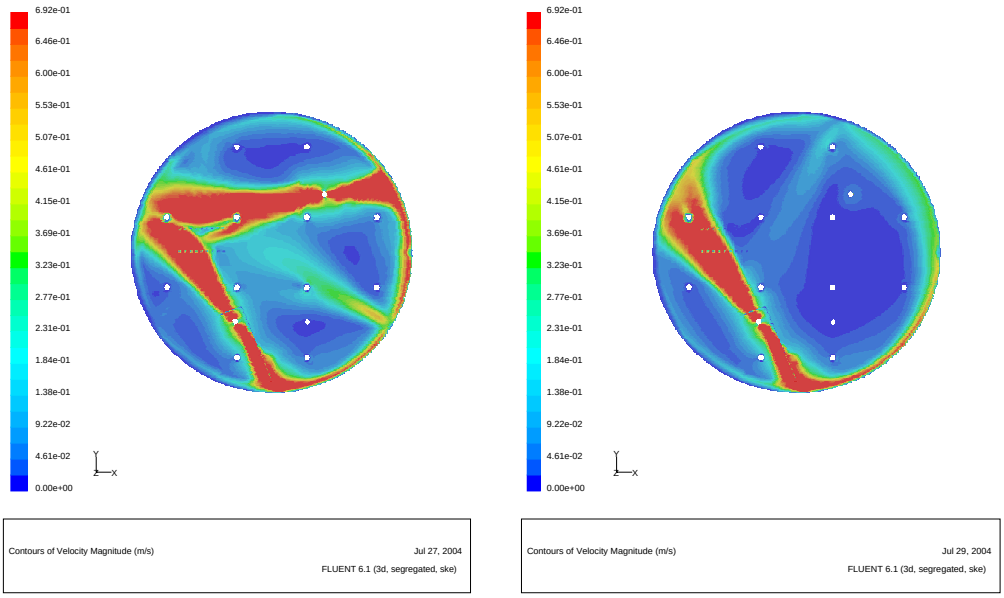

(Two-pump run: pumps no. 3 and no. 8) (One-pump run: pump no. 8)

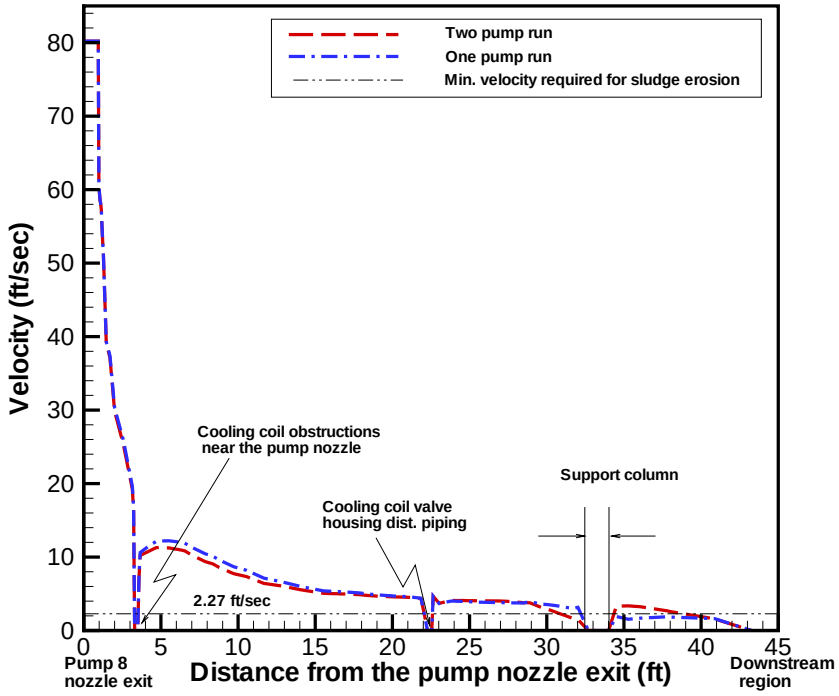

Figure 21. Comparison of velocity magnitudes between one-pump and two-pump runs along the principal discharge direction of pump no. 8 (The wall jet cases are for indexed operation ($\theta = 58^{o}$ in Fig. 20).)

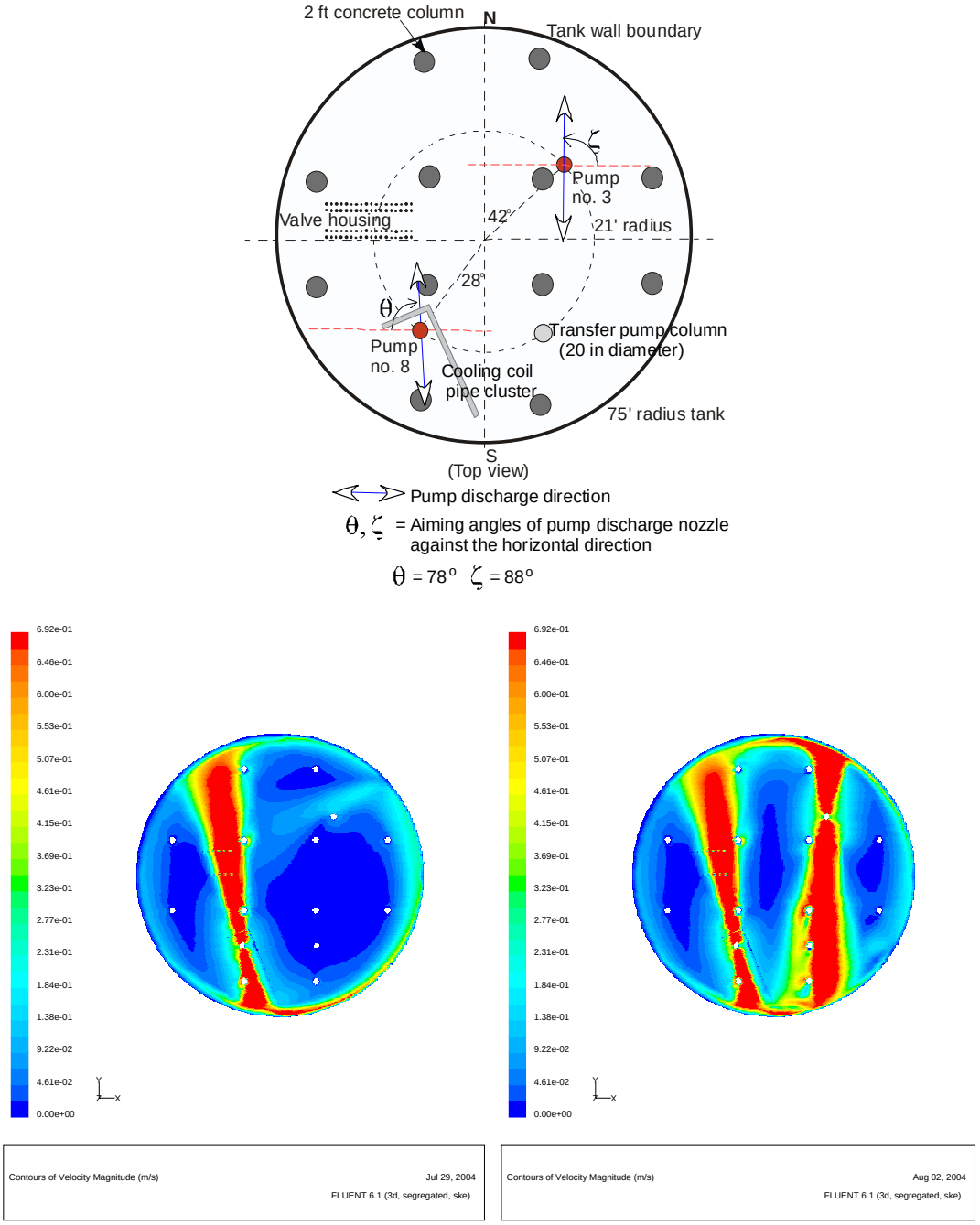

Figure 22. Comparison of flow patterns between one pump run with aiming angle of θ = 78° and two pump run with aiming angles of θ = 78° and ζ = 88° under the indexed mode operations showing that the red zone in the figure indicates the flow region larger than 2.27 ft/sec velocity magnitude

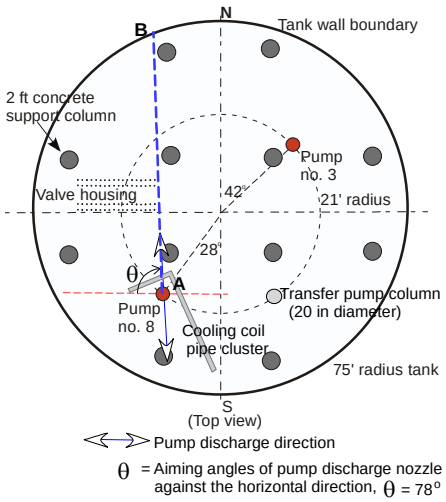

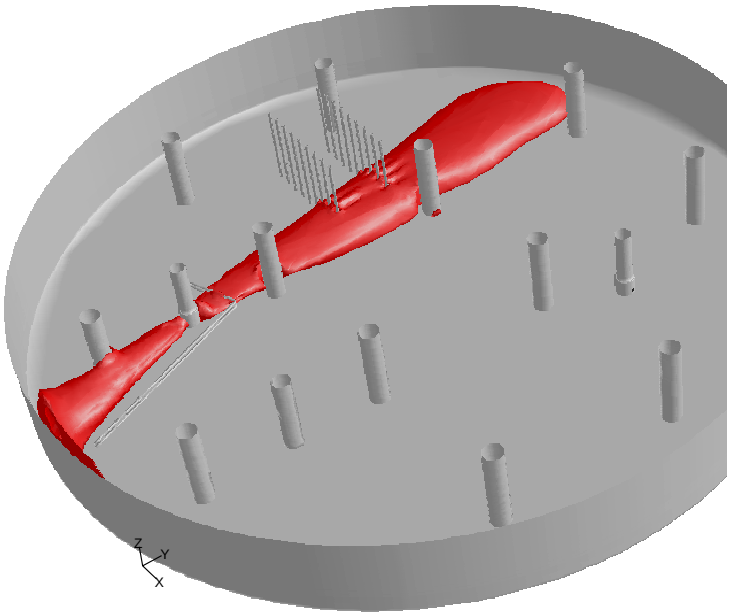

Figure 22a. Three-dimensional region of potential sludge erosion for one pump run with the most efficient aiming angle of $\theta = 78^{o}$ (as shown above) under the indexed mode operations showing that the red zone in the figure indicates the flow region larger than the minimum erosion velocity magnitude of 2.27 ft/sec

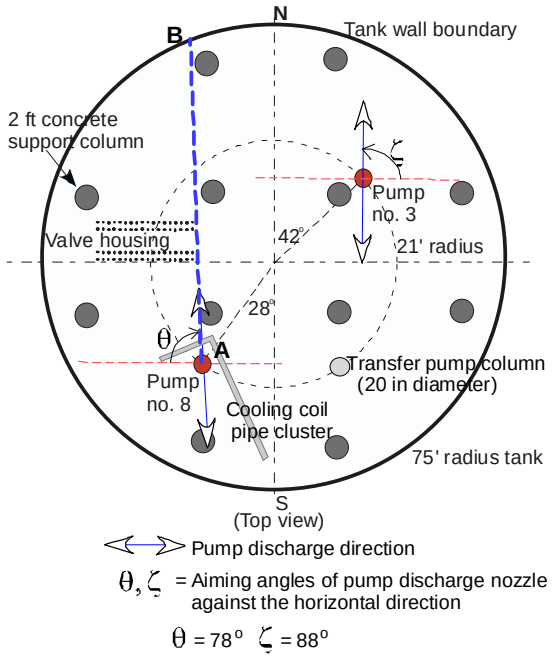

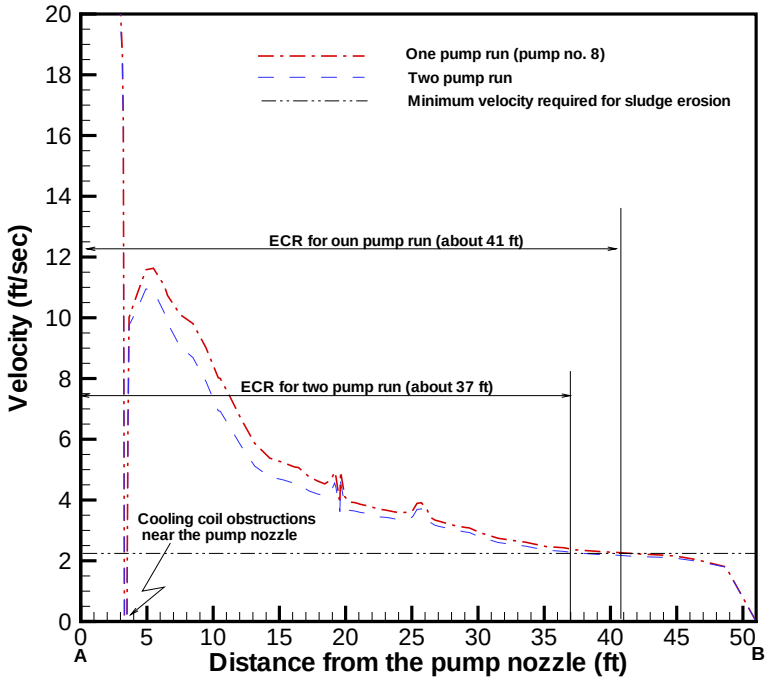

Figure 23. Quantitative comparison of local velocity magnitudes along the principal discharge line A-B of pump no. 8 between one pump run with aiming angle of $\theta = 78^{o}$ and two pump run with aiming angles of $\theta = 78^{o}$ and $\zeta = 88^{o}$ under the indexed mode run

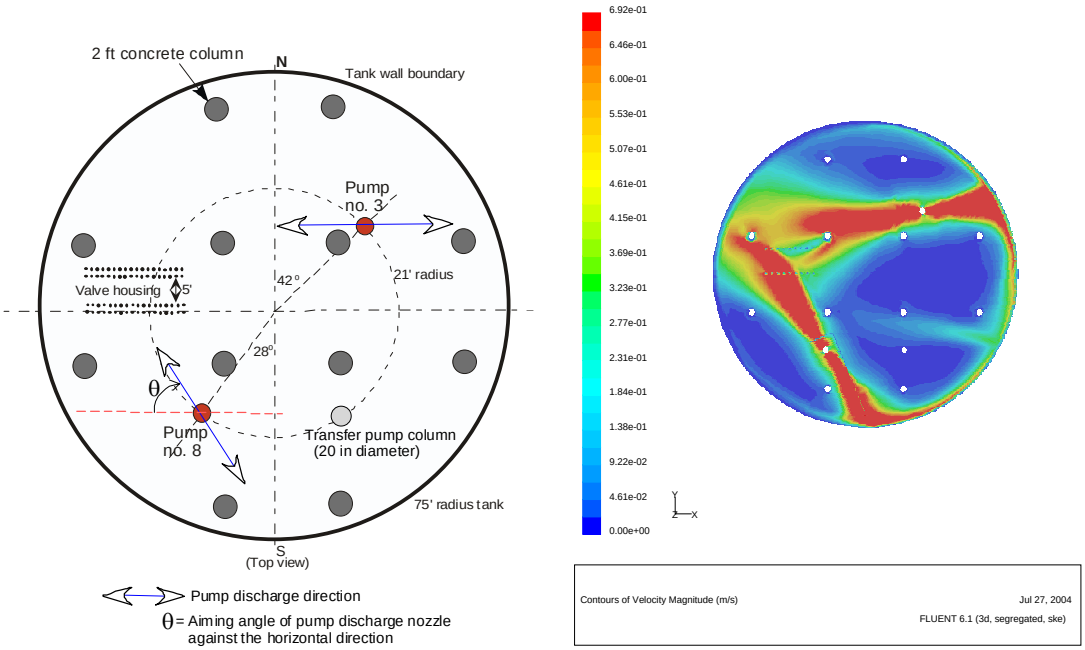

(45 in tank level)

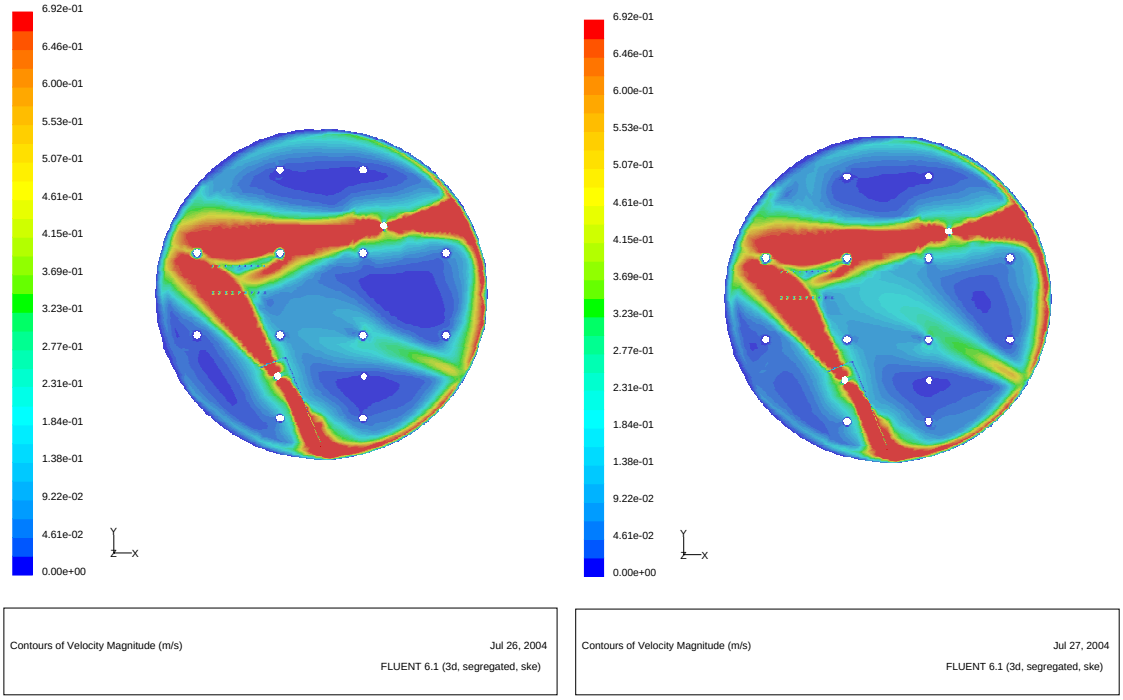

(70 in tank level) (101 in tank level)

Figure 24. Comparison of flow patterns at the nozzle exit plane of pump among three different tank levels under two pump run showing that red region indicates potential sludge removal region ($\theta = 58^{o}$)

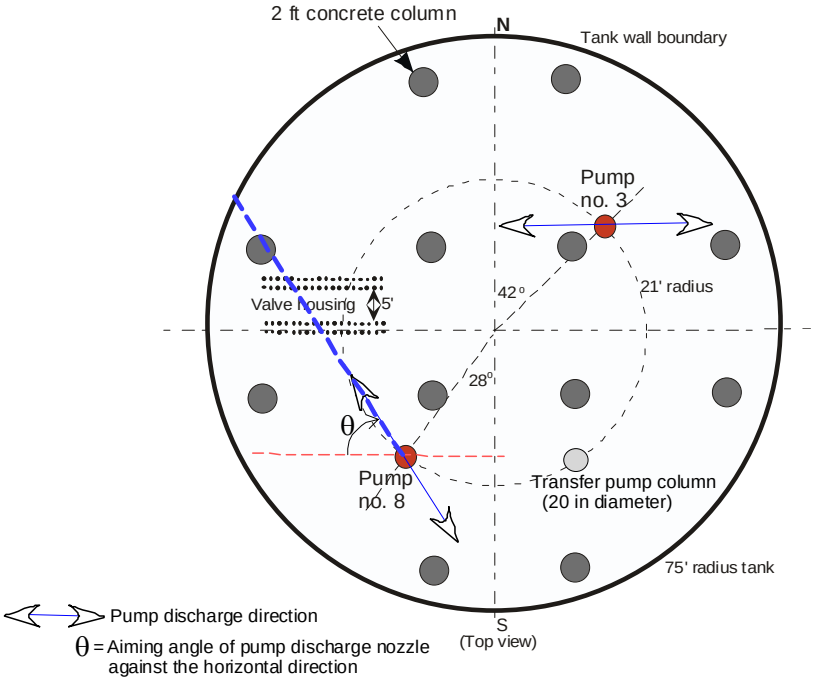

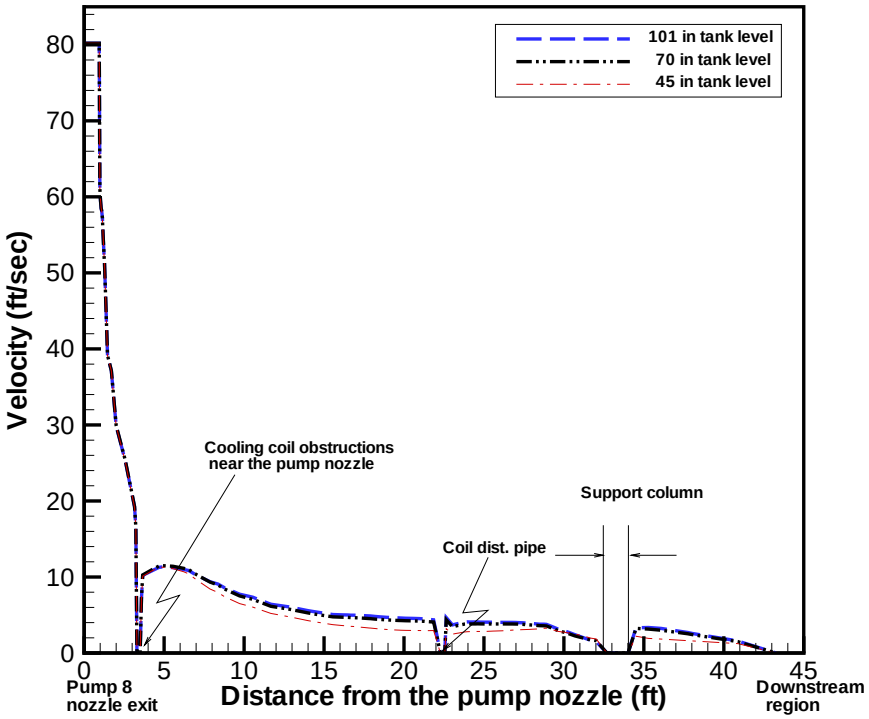

Figure 25. Comparison of local velocity magnitudes along the principal pump discharge directions pf pump no. 8 among three different tank levels under two pump run ($\theta = 58^{o}$)

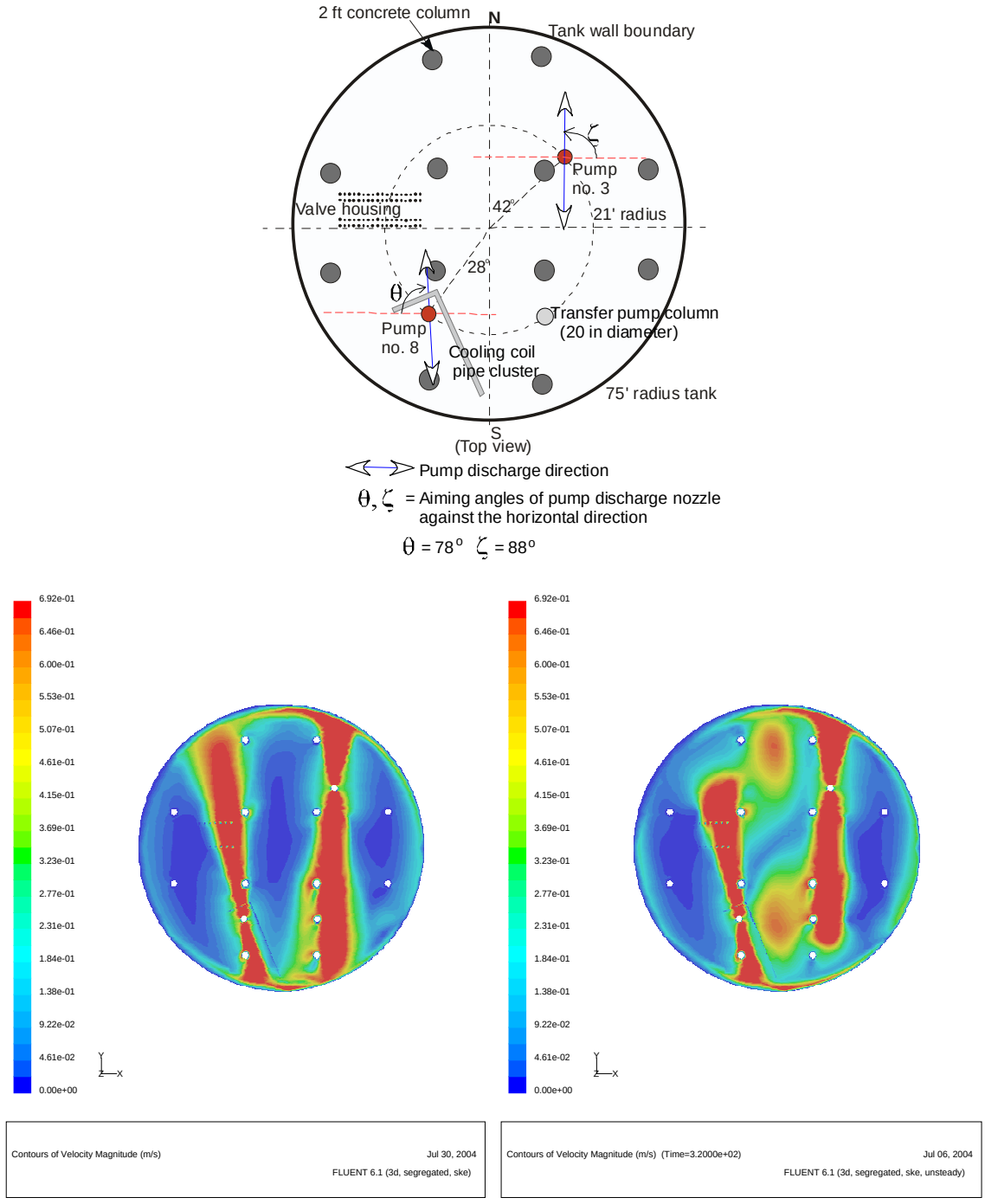

(Indexed mode) (Oscillating mode)

Figure 26. Comparison of flow patterns between indexed and oscillating operation modes under two-pump run with aiming angles of $\theta = 78^{o}$ and $\zeta = 88^{o}$ showing that the red zone in the figure indicates the flow region larger than 2.27 ft/sec velocity magnitude

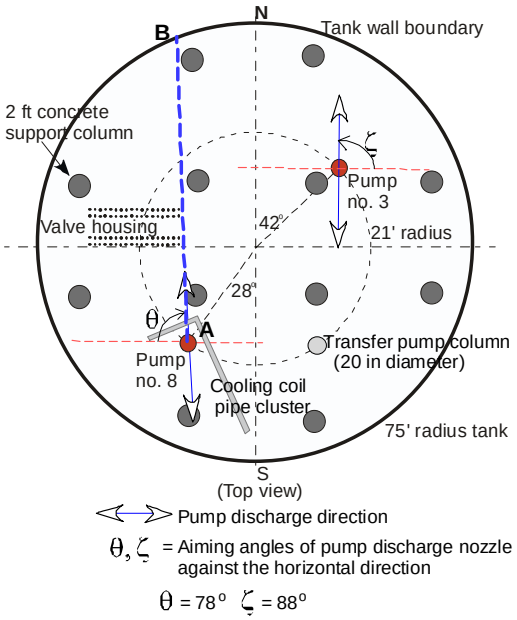

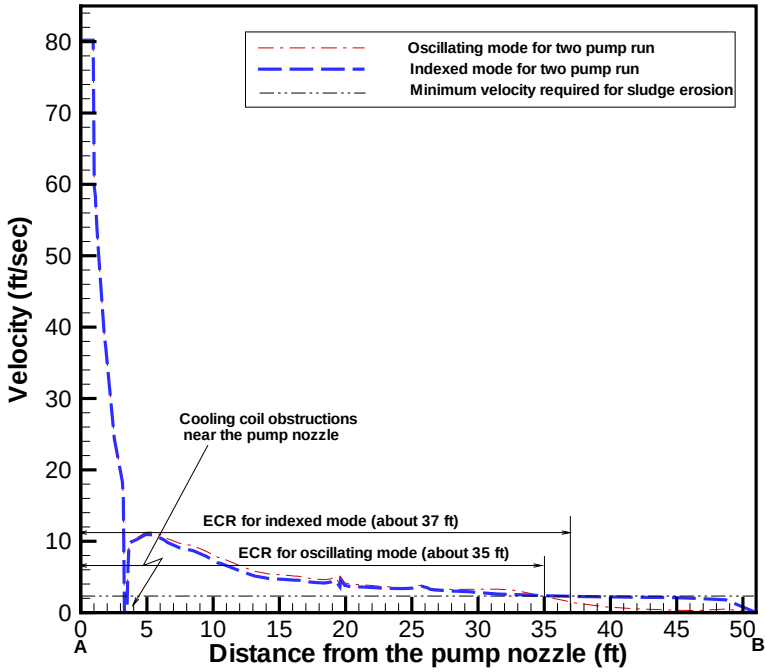

Figure 27. Quantitative comparison of local velocity magnitudes along the principal pump discharge direction between indexed and oscillating operation modes under two-pump run with aiming angles of $\theta = 78^{o}$ and $\zeta = 88^{o}$ showing that the red zone in the figure indicates the flow region larger than 2.27 ft/sec velocity magnitude

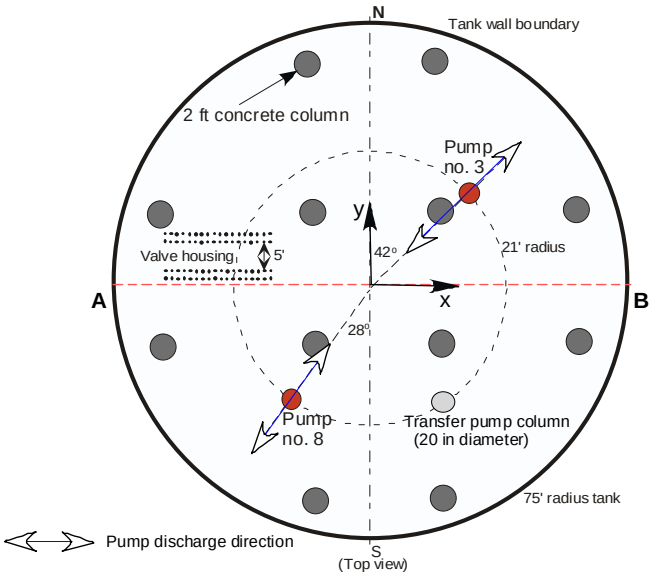

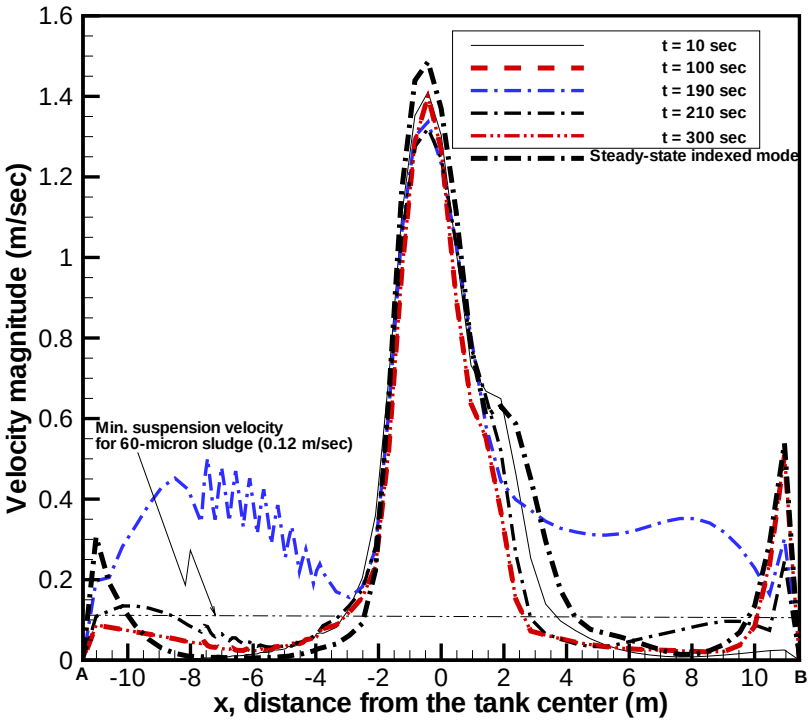

Figure 28. Comparison of local velocity magnitudes between oscillatory rotating and indexed pump operations for the pumps aiming at the tank center

Snapshots at t = 190 sec

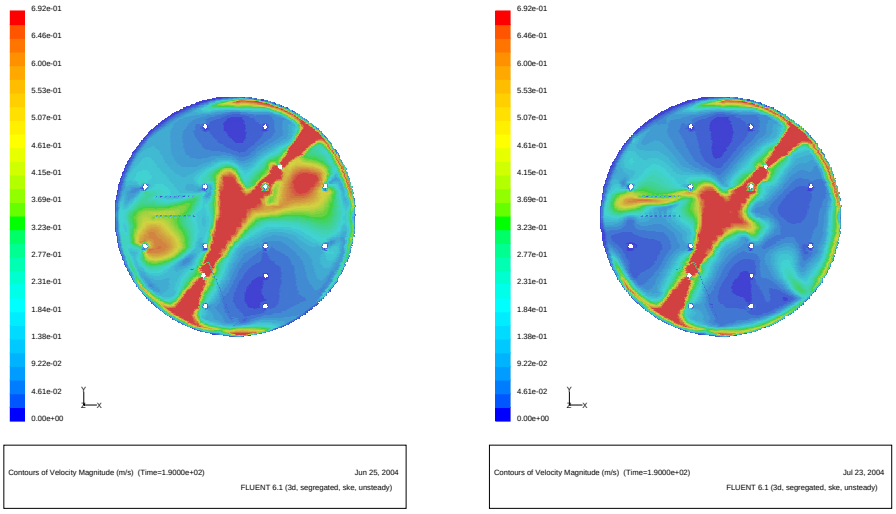

(Case A: Same direction for oscillation) (Case B: Opposite direction for oscillation)

Snapshots at t = 210 sec

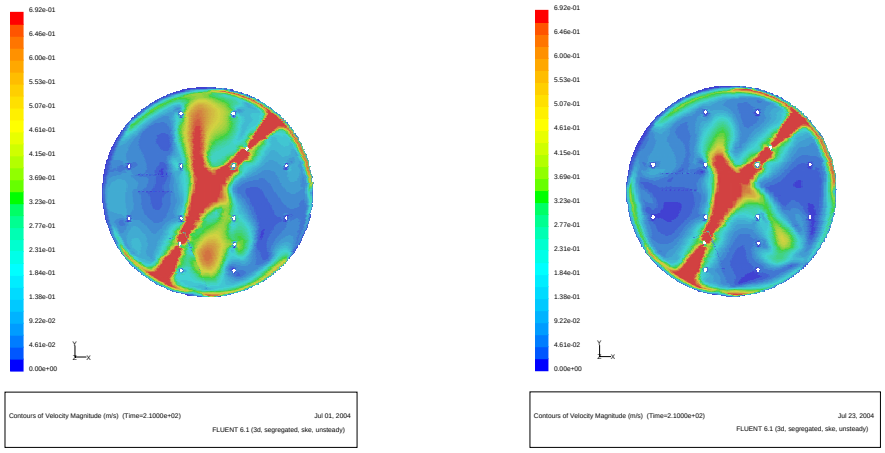

(Case A: Same direction for oscillation) (Case B: Opposite direction for oscillation)

Figure 29. Comparison of transient flow patterns between two different oscillating pump operations for the pumps aiming at the tank center

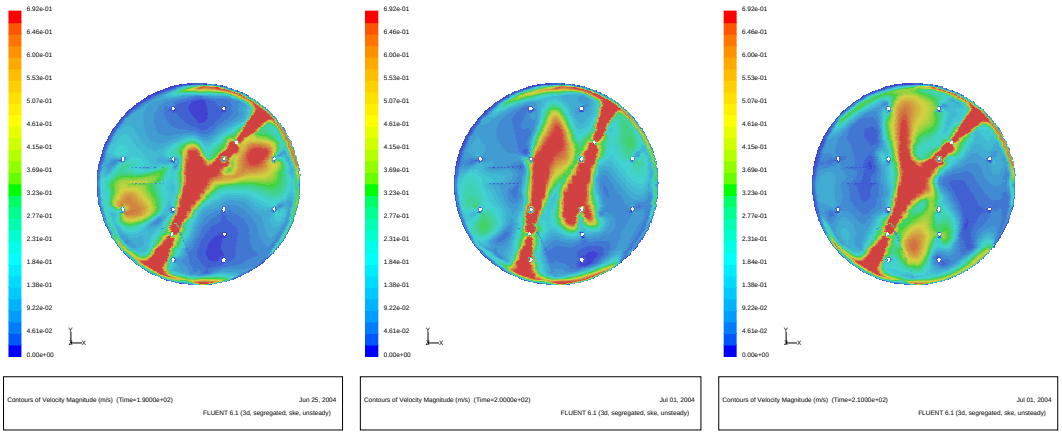

(t = 190 sec) (t = 200 sec) (t = 210 sec)

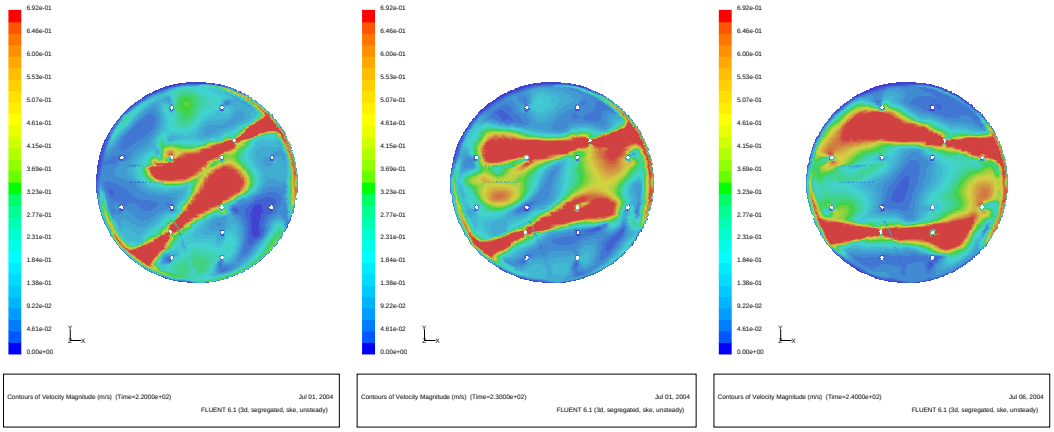

(t = 220 sec) (t = 230 sec) (t = 240 sec)

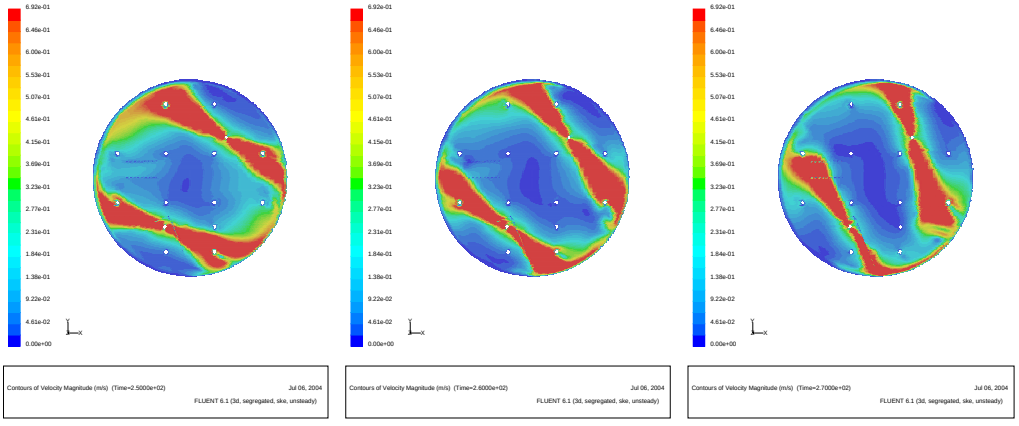

(t = 250 sec) (t = 260 sec) (t = 270 sec)

Figure 30. Quasi-steady flow patterns for $\pm 200^{o}$ oscillating mode with the same rotating direction (Case A) under two pump run showing that the red region indicates the zone larger than 0.6918 m/sec (2.27 ft/sec) erosion velocity

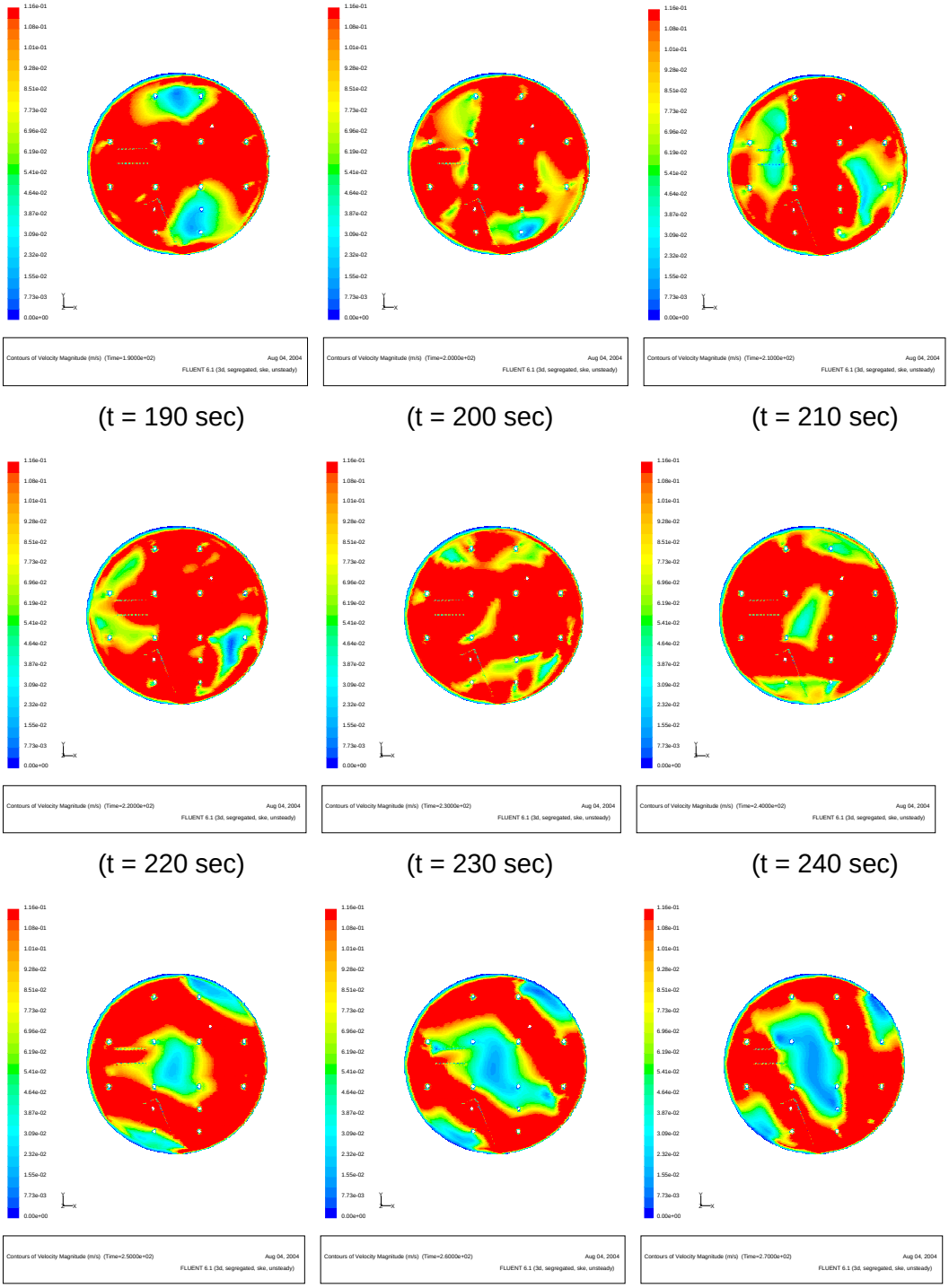

Figure 31. Quasi-steady flow patterns for $\pm 200^{o}$ oscillating mode with the same rotating direction (Case A) under two pump run showing that the red region indicates the zone larger than 0.116 m/sec (0.380 ft/sec) suspension velocity of 60 micron sludge particle

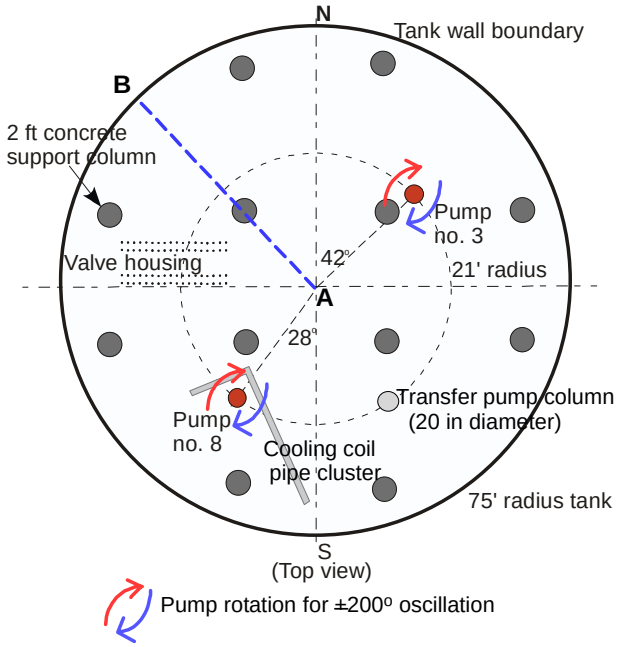

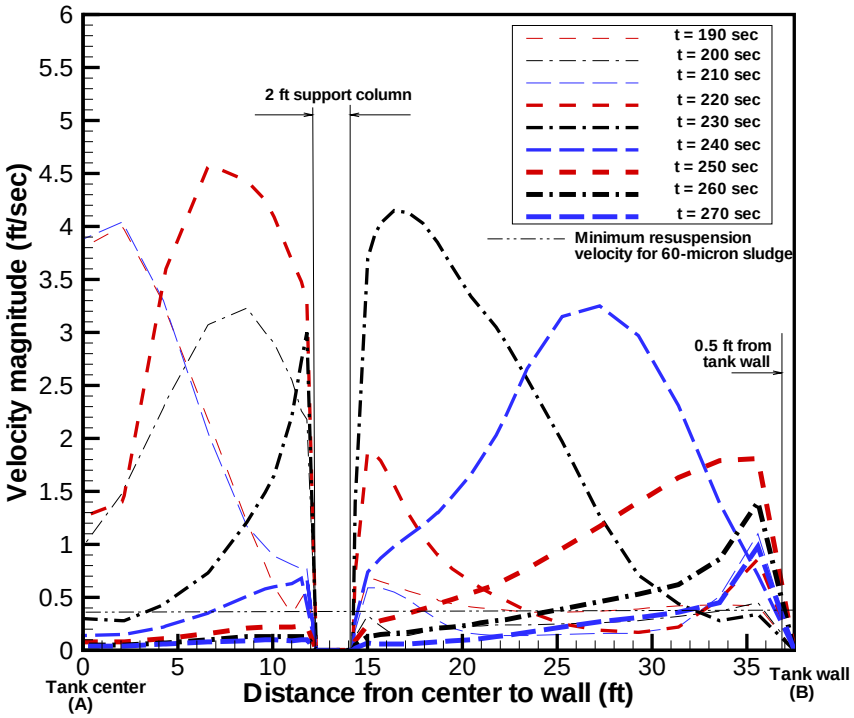

Figure 32. Quasi-steady velocity magnitudes along the line A-B for $\pm 200^{o}$ oscillating mode with the same rotating direction (Case A) under two pump run showing suspension velocity of 60 micron sludge particle (0.380 ft/sec as shown in Table 3)

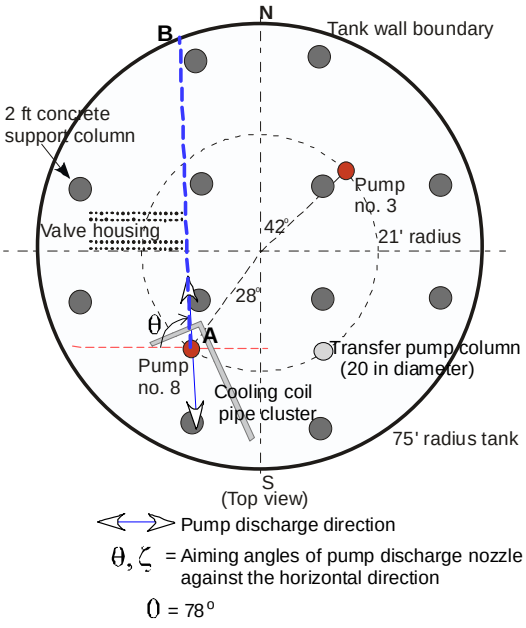

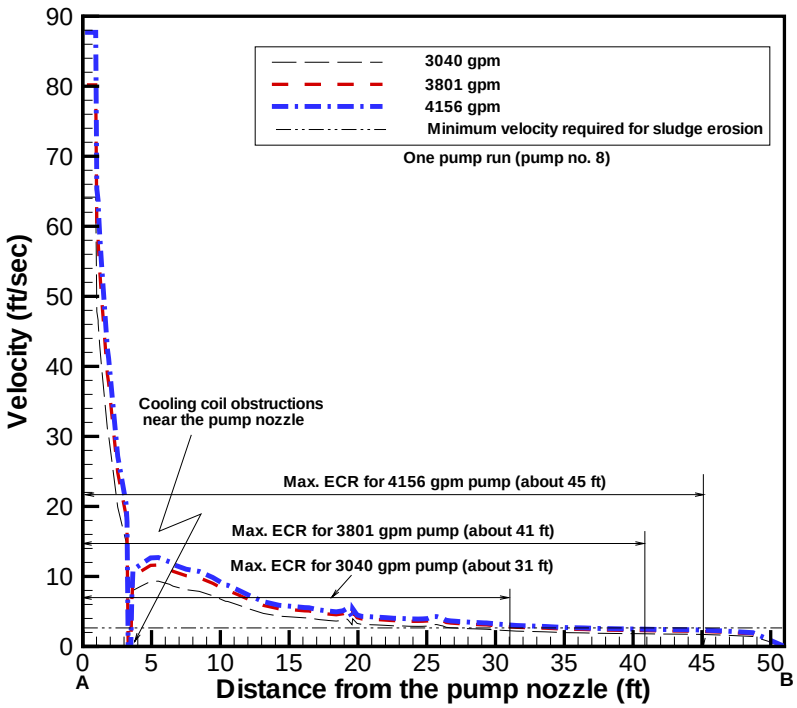

Figure 33. Quantitative comparison of local velocity magnitudes and maximum ECR's along the principal pump discharge directions of pump no. 8 among three different pump flowrates of 3040 gpm, 3801 gpm, and 4156 gpm under one pump run ($\theta = 88^{o}$)

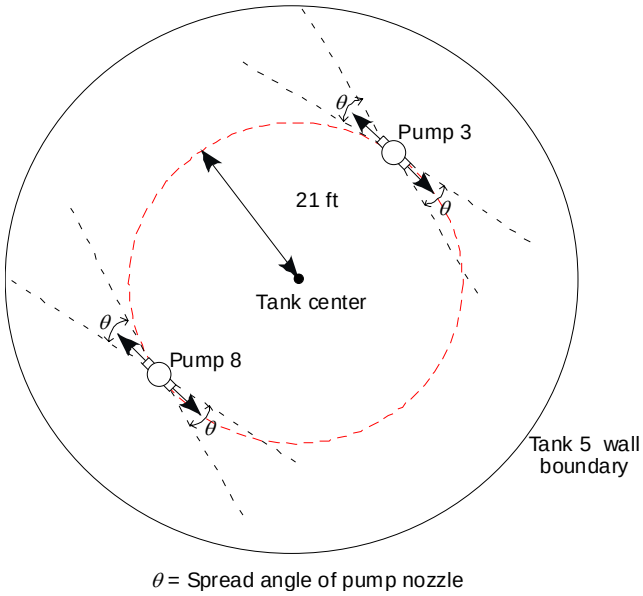

Figure 34. Spread angle evolved by the momentum dissipation of submersible mixing pump inside the wall boundary of Tank 5 ($\theta \approx 14^{o}$)

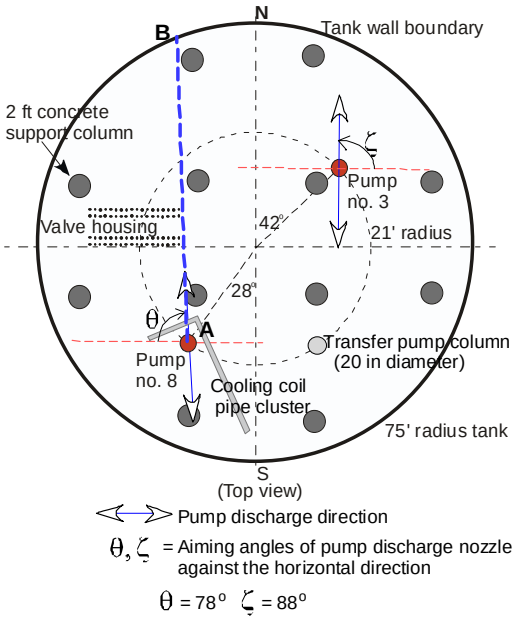

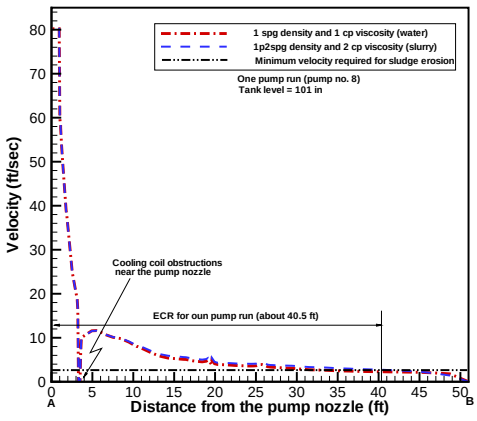

(One pump run of pump no. 8)

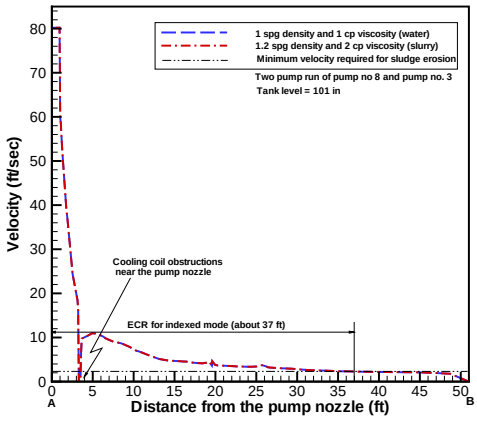

(Two pump run of pump no. 8 and no 3)

Figure 35. Comparison of local velocity magnitudes along the principal pump discharge directions pf pump no. 8 between water and potential slurry fluid under one-pump and two-pump runs

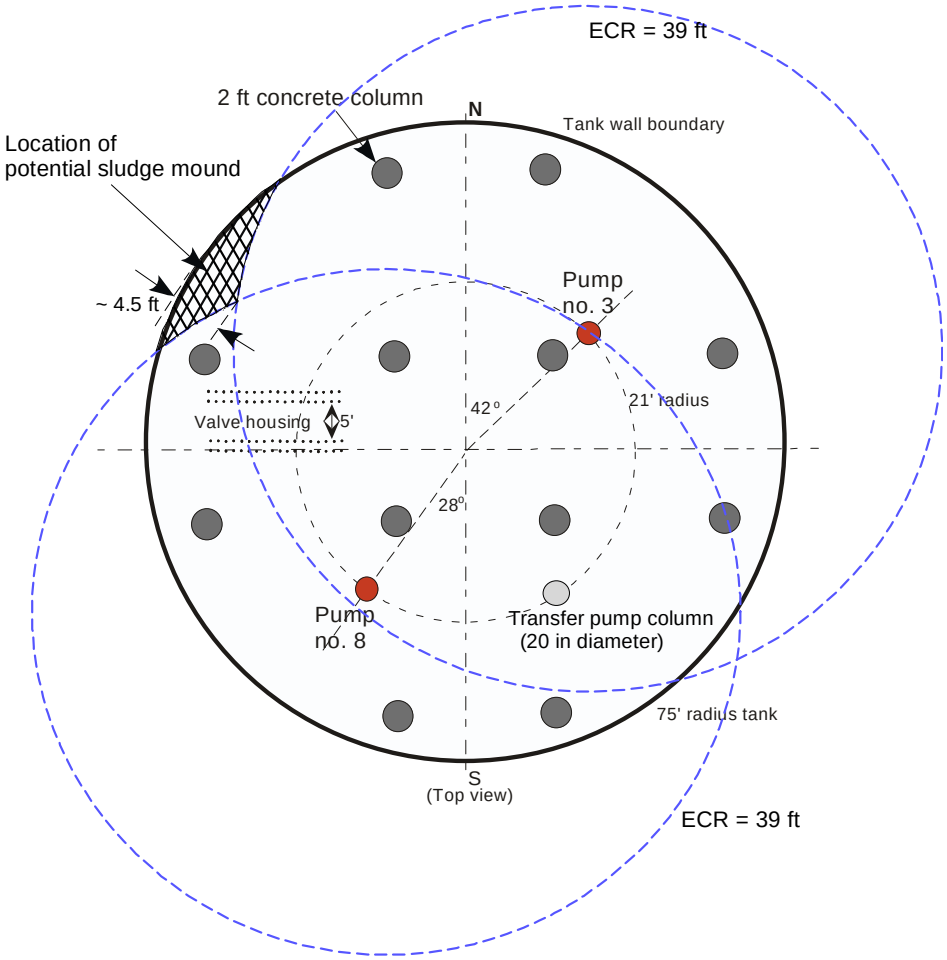

Figure 36. Predictions of sludge removal domain provided by the indexed nominal operations of two mixing pumps for the reference pump flowrate (3801 gpm per nozzle)

4. Summary and Conclusions

Tank 5 simulation models with two submersible slurry pumps have been developed to provide operational guidance of slurry pumps for an efficient sludge removal. Sensitivity calculations for different tank levels and pump flowrates have been performed to provide an operational input for sludge heel suspension and removal in Tank 5. Reference design and operating conditions shown in Table 2 were used to perform the best estimate analysis of the tank sludge removal. In the analysis, the pump was assumed to be stationary or oscillating as requested by the customer [2]. Major solid obstructions including the pump housing, the second SMP pump column, twelve 2-ft concrete support columns, one submersible transfer pump riser and 2-in cooling pipe clusters were included in the present model. Free surface motion of the tank liquid was neglected for high tank liquid level following the previous work [6].

Steady-state and transient analyses with a two-equation turbulence model were performed with FLUENT^{TM}, a commercial computational fluid dynamics (CFD) code. All analyses were based on three-dimensional results. A recommended operational guidance was developed assuming that local fluid velocity can be used as a measure of sludge suspension and removal. For a minimum suspension velocity of 2.27 ft/sec, the results indicated that the existing slurry mixers running at 3801 gpm could remove the sludge heel from the tank with a 101 in liquid level. In this case, the exception is the region within about 4.5 ft of the wall, which is located behind the support columns near the west corner of the tank. The results also show that a tank liquid level higher than 70 inches does not have any impact on the effective cleaning distance.

The main conclusions drawn from the Tank 5 modeling and calculations are as follows:

- Internal obstructions such as the 2-ft support columns under two-pump run can help guide local flow velocity into some regions where potential sludge heel is located in Tank 5.
- When twelve concrete columns are present as flow obstructions inside the tank, maximum clearing distance of the slurry mixer from an indexed pump position for the one-pump run is found to be about 41 ft assuming the minimum velocity required to suspend waste sludge is 2.27 ft/sec.
- It is noted that the higher pump flowrate is generally more efficient than the lower in terms of sludge removal capability, but it is about the same in terms of flow circulation patterns. When pump flowrate is lower than 3801 gpm, the velocities near the wall region are probably not high enough to suspend and mobilize the sludge.
- Under indexed pump operation, the major impact of the results for the presence of the 2-ft support columns is that the sludge cleaning distance is reduced by about 1.5 ft, compared to the pump orientation without any flow obstructions along the principal discharge direction of the pump nozzle. However, the impact of the cleaning distance for the presence of 2-in cooling coil pipe clusters near the pump nozzle is found to be negligible.
- Indexed pump operation has better ECR performance, compared to the oscillation mode of pump operation. However, the oscillating operation mode provides broader cleaning area.

- Under oscillating pump operation, two pumps run with same rotating directions has a better mixing efficiency, compared to the one with opposite rotating directions

These analysis results performed by the present models will be used to evaluate hydraulic cleaning capabilities for new submersible mixer pump and to provide a recommended operational guidance for Tank 5 waste removal. This information will also assist in the operating plan for the Tank 5 waste removal and in identifying special operation requirements for the suspension and removal of the tank sludge heel.

6. References

1. J. M. Jenkins, “Tank 5 Waste Removal Operating Plan”, CBU-LTS-2003-00135, Rev. 0, March 2004.
2. Technical Task Request by Jwalit J. Purohit, “Submersible Mixer Pump (SMP) Computational Fluid Dynamics (CFD) Modeling”, HLW-TTR-2004-064, January 14, 2004.
3. Personal Communications with T. M. Punch on Tank 5 Cooling Coil Pictures and Detailed Internal Configurations, March 22, 2004.
4. V. M. Cordaro, “SMP Dimensions”, e-mail, May 13, 2004.
5. S. Y. Lee and R. A. Dimenna, “Performance analysis for Mixing Pumps in Tank 18”, WSRC-TR-2001-00391, October 2001.
6. S. Y. Lee, R. A. Dimenna, R. A. Leishear, and D. B. Stefanko, “Mixing in Large Scale Tanks Part I; Flow Modeling of Turbulent Mixing Jets”, HT-FED2004-5622, 2004 ASME Heat Transfer / Fluids Engineering Summer Conference, Charlotte, N. C., July 11-15, 2004
7. S. Y. Lee, “Updated Tank 11 Model for Sludge Heel Removal Analysis”, WSRC-TR-2004-00099, March 2004.
8. S. Y. Lee, “Evaluation of Sludge Removal Capabilities for ADMP Mixer in Tank 18, WSRC-TR-2003-00166, April 2003.
9. *FLUENT*, Fluent, Inc., 1998.
10. G. Tatterson, “Sludge Suspension in Waste Storage Tanks”, DPST-89-257, January 6, 1989.
11. G. Tatterson, “Jet Mixing in In-Tank Processing (U)”, DPST-89-380”, DPST-89-380, January 24, 1989.
12. W. H. Graf, *Hydraulics of Sediment Transport*, McGraw-Hill Book Company (1971).
13. J. M. Dallavalle, *Micromeritics*, 2nd Edition, Pitman Publishing Corporation, New York (1948).
14. Abramovich, G. N., “*The Theory of Turbulent Jets*”, The MIT Press, Cambridge, MA, 1963.
15. N. V. Chadrasekhara Swamy and P. Bandyopadhyay, “Mean and Turbulence Characteristics of Three-Dimensional Wall Jets”, *Journal of Fluid Mechanics*, Vol. 71, Part 3, pp. 541-562 (1975).

(This Page Intentionally Left Blank)